Environmental Microbiology

ENVIRONMENTAL MICROBIOLOGY

RESEARCH ARTICLE OPEN ACCESS

Symbiodiniaceae and Bacterial Microbiome Dynamics Differentially Impact the Survival of Dominant Reef-Flat *Porites* Corals

Colin Lock[1,2] | Therese C. Miller[1,3] | Colin J. Anthony[1,4] | Héloïse Rouzé[1,5] | James Fifer[6] | Grace McDermott[1] | Carlos A. Tramonte[1] | Loreto Paulino Jr[1] | Sarah W. Davies[6] | Laurie Raymundo[1,7] | Bastian Bentlage[1]

[1]Marine Laboratory, University of Guam, Mangilao, Guam, USA | [2]Climate Change Cluster, University of Technology Sydney, Ultimo, New South Wales, Australia | [3]Institute of Marine Science, University of Auckland, Auckland, New Zealand | [4]Department of Integrated Biosciences, Graduate School of Frontier Sciences, The University of Tokyo, Chiba, Japan | [5]MARBEC, Univ Montpellier, CNRS, Ifremer, IRD, Dembeni, Mayotte | [6]Department of Biology, Boston University, Boston, Massachusetts, USA | [7]James Cook University, Townsville, Australia

Correspondence: Colin Lock (clockdive@gmail.com) | Bastian Bentlage (bentlageb@triton.uog.edu)

Received: 20 January 2025 | **Revised:** 25 August 2025 | **Accepted:** 29 August 2025

Funding: This work was directly supported by Guam NSF EPSCoR through the National Science Foundation (award OIA-1946352).

Keywords: acclimatisation | bacteria | coral restoration | *Endozoicomonas* | *Parendozoicomonas* | *Porites* | Symbiodiniaceae

ABSTRACT

Coral reefs face significant threats across the globe, prompting a surge in restoration efforts aimed at mitigating their global decline. The health, resilience, and adaptability of corals are greatly influenced by their microbial communities, and while the response of coral microbiomes to many environmental stressors has been extensively studied, less is known about their natural dynamics following transplantation, which is an essential process for restoring degraded reef habitats. In this study, we integrated DNA metabarcoding (16S & ITS2) with ecological monitoring to investigate the dynamics of Symbiodiniaceae and bacterial communities in two dominant coral spp., *Porites lobata* and *Porites cylindrica*, and their different colour morphs, as they underwent transplantation and an 18-week acclimatisation period. We saw significant differences in microbial communities between the two *Porites* spp., outplanting sites, and individual coral colonies, as well as a colour morph-related difference in *P. lobata* bacterial communities. We saw reduced relative abundances of *Endozoicomonadaceae,* specifically from the genus *Parendozoicomonas,* following transplantation. *P. lobata* colonies with later Symbiodiniaceae shifts (18 weeks) had lower long-term survival. Changes in Symbiodiniaceae and bacterial communities have implications for holobiont function and colony survival, which should be considered when designing and implementing coral reef rehabilitation projects.

1 | Introduction

1.1 | Coral Reef Restoration

Corals are complex holobionts that rely on interactions with several symbiotic microorganisms, including dinoflagellate algae (Symbiodiniaceae) and a diverse bacterial community. These coral holobionts provide the basis for one of earth's most productive and diverse ecosystems (Knowlton et al. 2010), which directly supports the livelihoods of millions of people (Cinner 2014). However, increasing sea surface temperatures are threatening coral reefs, in particular by disrupting the relationship between corals and their Symbiodiniaceae endosymbionts (Hughes et al. 2017). Coral species and their associated microbial communities exhibit variation in their ability to acclimate to new conditions through phenotypic and physiological plasticity

(e.g., Maor-Landaw and Levy 2016; Anthony, Lock, et al. 2023), shuffling of algal symbionts (e.g., Cunning et al. 2015), and maintenance of beneficial bacterial communities (e.g., Epstein et al. 2019; Grottoli et al. 2018; Ziegler et al. 2017). However, there are limits to this acclimatisation potential, which has resulted in major losses of coral diversity and coverage worldwide (Hughes et al. 2017).

Interest in coral reef restoration has increased in recent years to attempt offsetting global losses in coral coverage, which has been estimated as high as 50% compared to a 1950s baseline (Boström-Einarsson et al. 2020). Restoration aimed at mitigating acute disturbances (e.g., port dredging, ship groundings, storm damage) can have lasting impacts, but the impacts of chronic stressors such as rising sea surface temperatures, along with species-specific responses of corals need to be considered for restoration efforts to be sustainable (Boström-Einarsson et al. 2020). Common garden and transplantation experiments have tested the suitability of restoration sites and the acclimatisation potential of coral species (Epstein et al. 2001; Kenkel et al. 2013; Tisthammer et al. 2021), but further work is needed to elucidate the shifts of coral-associated microbial communities and understand their influences on coral health and resilience (van Oppen and Blackall 2019; Voolstra et al. 2024). The application of probiotics and other microbiological interventions has even been proposed as a means to increase the success of coral restoration projects (Li et al. 2022). However, understanding the dynamics and persistence of coral-associated symbionts and bacterial microbiome communities is an important first step prior to developing coral restoration strategies that utilise manipulation of these communities.

1.2 | Microbiome Underpins Coral Health and the Success of Restoration

In recent decades, there has been a growing awareness of the connection between development, metabolism, and health of animals and their microbiomes. Specifically, the coral-Symbiodiniaceae symbiosis provides much of the energetic requirements for most tropical, scleractinian corals. A plethora of studies have documented functional trade-offs between different clades of Symbiodiniaceae for the coral holobiont (e.g., Berkelmans and Van Oppen 2006; Hoadley et al. 2021; Stat et al. 2008; Xiao et al. 2022), host-specificity of Symbiodiniaceae (e.g., Hume et al. 2020), plasticity in Symbiodiniaceae communities (e.g., Cunning et al. 2015), and phenotypic plasticity across space and time (Anthony, Lock, et al. 2023). In the context of coral restoration, understanding the stability of Symbiodiniaceae communities and the ability of different symbiont clades and genotypes to tolerate adverse conditions can affect the success of restoration projects (Nitschke et al. 2024).

Coral-associated bacteria provide various beneficial functions to the coral host ranging from nutrient cycling (Ceh et al. 2013; Raina et al. 2009) and antimicrobial defence (Shnit-Orland and Kushmaro 2009) to increased thermal tolerance (Gilbert et al. 2012). However, bacteria are also responsible for diseases that may lead to partial or complete colony mortality (Vega Thurber et al. 2009). Therefore, the bacterial microbiome community can have a profound impact on coral health, acclimatisation potential, and, by extension, coral restoration success (Moriarty et al. 2020). While some corals exhibit flexibility in their microbial associations ('microbiome conformer'), other coral species maintain stable microbiomes ('microbiome regulator') through time and environmental stress (Ziegler et al. 2019). Stable coral bacterial communities have been observed in colonies that survive bleaching events (Epstein et al. 2019; Grottoli et al. 2018; Ziegler et al. 2017), while bacterial dysbiosis, or the imbalance of the bacterial microbiome, has been linked to coral bleaching (Bourne et al. 2008), compromised host immune systems (Pinzón et al. 2015), and disease outbreaks (Casey et al. 2015). While the coral-associated bacterial microbiome remains poorly understood and understudied, it represents a crucially important component of coral health and resilience. Effective management and restoration of coral reefs will thus benefit from understanding bacterial microbiome community dynamics such as species turnover in response to transplantation. Can corals maintain potentially beneficial microbiomes following transplantation to a novel restoration site? Does dysbiosis persist or do coral microbiomes return to a homeostatic state?

1.3 | *Porites* as a Study Genus and Functional Trade-Offs of Coral Colour Morphology

Corals from the genus *Porites* represent dominant reef-building corals across the Indo-Pacific and account for up to 80% of total live coral cover at several sites around Guam, making them important contributors to reef structure (Burdick et al. 2023). Due to their global importance, several *Porites* species have been used for coral restoration efforts globally and locally around Guam (Forsman et al. 2006; Cabaitan et al. 2015; Lock et al. 2022). The slow-growing nature of *Porites* spp. is a challenge for restoration but makes them ideal candidates for exploring and implementing microfragmentation techniques, which have been shown to increase the growth rate of slow-growing massive corals (Page et al. 2018). Furthermore, *Porites* spp. are generally regarded as relatively resilient to stressors such as elevated seawater temperatures (Raymundo et al. 2019) and sedimentation (Lock et al. 2024; Golbuu et al. 2011), making them ideal candidates to restore degraded reefs which often experience harsh conditions. Among *Porites* genera and species, several morphologies and life history strategies exist. Some species are resilient, slow-growing massive corals, such as *Porites lobata*, whereas others, like *Porites cylindrica*, exhibit a branching morphology. Interestingly, *Porites* corals are widely considered to be microbiome regulators that maintain consistent endosymbiotic diversity across environmental gradients and through environmental change (Stat et al. 2009; Barshis et al. 2010; Putnam et al. 2012). Yet, the microbiome's response to transplantation within this genus has not been well explored. In general, *Porites* spp. are less susceptible to environmental stressors compared to many other coral genera and may represent an important group for restoration efforts to preserve ecosystem functions in a rapidly changing climate.

Porites lobata and *P. cylindrica* exhibit colour polymorphism (Anthony, McDermott, Lock, et al. 2023), which has been associated with functional trade-offs in disease (Shore-Maggio et al. 2015), bleaching susceptibility (Satoh et al. 2021), and

microbiome composition (Shore-Maggio et al. 2015; Lesser et al. 2019) in other coral species. Furthermore, differences in distributions have been documented for colour morphs of *Porites* spp. For example, *P. astreoides* colour morph distributions have been shown to vary across gradients of sedimentation and depth, suggesting that coral colour can influence light attenuation and, in turn, impact Symbiodiniaceae endosymbionts (Gleason 1998, 1993). In Guam, massive *Porites* (including *P. lobata*) are most commonly observed in purple and brown colour morphologies but can transition between them (Anthony, McDermott, Lock, et al. 2023), whereas *P. cylindrica* colonies are generally brown or yellow in colour. Colour morphs co-occur on Guam's reef flats and no structuring across depth gradients on the fore-reef has been observed to date (Anthony, McDermott, Lock, et al. 2023). Based on the functional differences observed between colour morphologies in other coral species, we investigated whether there were underlying differences in the microbial communities of *Porites* spp. and what influence this might have on restoration success.

The resilience of *Porites* spp., and their important role as reef-builders in Guam and across the Pacific, makes *Porites* a genus of interest for preserving reef ecosystem services under future climate scenarios. Our aim was to understand the response of *P. lobata* and *P. cylindrica* microbiome communities to in situ transplantation and 18 weeks of acclimatisation using a common garden approach. Symbiodiniaceae cell densities were estimated using flow cytometry to identify possible changes in symbiont densities following transplantation and subsequent acclimatisation to their new environment. DNA metabarcoding was employed to investigate microbiome community shifts of Symbiodiniaceae and bacteria. Transplanted corals were monitored for disease and partial mortality to link possible differences in transplantation success to microbiome community shifts. Since we did not monitor the microbial communities of corals from the donor site, it is difficult to untangle whether these changes arose because of transplantation or a combination of factors, including natural temporal dynamics. Yet, we maintain the use of the word transplantation for simplicity when discussing the temporal component of our study. However, we focus our discussion on the microbial differences between *Porites* spp., colour morphologies, and the common garden sites, as well as how these differences were correlated with restoration outcomes, specifically partial mortality of coral fragments.

2 | Methods

2.1 | Common Garden Setup

To identify differences in community dynamics of Symbiodiniaceae and bacterial community assemblages, two colour morphs of two species of *Porites* (brown *P. cylindrica*, yellow *P. cylindrica*, brown *P. lobata* and purple *P. lobata*) were collected from the Luminao reef flat and transplanted directly to cleaned areas of limestone pavement to establish four common garden plots at two sites (Piti-West, Piti-East) within Piti Marine Preserve, Guam (Figure 1A). Piti Marine Preserve was selected as the transplantation site as it had similar environmental conditions (temperature, water depth, water flow dynamics) and coral species compared to Luminao and was located within a marine protected area to avoid disruption over the course of the experiment. Ten colonies for each coral species/colour morph ($n = 40$ total) were collected from the Luminao reef flat and carefully subdivided into eight clonal fragments of ~15 cm size each ($n = 80$ for each species/colour morph; Figure 1A). Fragments were transplanted across the four common garden plots in the Piti Marine Preserve by attaching them directly to the substrate in a grid layout, with approximately 10 cm between each colony, using A-788 Splash Zone Epoxy (Pettit Paint, Rockaway, NJ), assigning placement of each coral fragment in common garden plots at random (see Figure S1 for an example layout). *Porites* colonies were transplanted side by side with *Acropora pulchra* fragments, which we described in another publication (Anthony, Lock, Pérez-Rosales, et al. 2024). In each plot, two replicate fragments of each species/colour morph were transplanted side by side for a total of 80 fragments transplanted at each site. One fragment was left intact to be monitored for health impacts, and the second was assigned for repeat sampling of tissues for microbiome assessment.

2.2 | Environmental Data Collection, Monitoring, and Sampling

Environmental data were gathered continuously at 15-min intervals using loggers that record temperature, light (HOBO pendant temperature/light, model: UA-002-64, Onset Corporation Bourne, MA), and water depth (HOBO water level data logger, model: U20L-01, Onset Corporation Bourne, MA) at the substrate level in the centre of each common garden plot (Figure S2). Water depth was measured using loggers that recorded absolute pressure in kPa; absolute pressure was converted to water depth after correcting recorded pressure values for variations in air pressure that were recorded at sea surface level near the Piti Marine Preserve using a HOBO water level data logger deployed on land. As part of the initial common garden site characterisation, water samples were taken during the transplantation timepoint (Week 4) to record orthophosphate, nitrite, and nitrate concentrations in the water column; these parameters were determined using the commercial analytical services of the Water and Environmental Research Institute of the Western Pacific (WERI) at the *University of Guam*.

Transplanted corals in the common garden plots were monitored for signs of disease and mortality seven times (~every 2 weeks) from May 11, 2021 to October 12, 2021. During this period, grayscale-normalised photographs were taken to track colour fluctuation of corals following transplantation. These were then used to quantify coral colour intensity (CCI) as described in the publicly available, step-by-step protocol (Paulino Jr. et al. 2023). To account for the effects of colour morph pigmentation, we fitted colour morph-specific repeated-measures ANOVAs, with individual colony IDs included as random effects, to better detect bleaching patterns driven by spatio-temporal factors, as implemented in base R v4.2.2 (Team RC 2013). Residuals were assessed for normality using the Shapiro–Wilk test and transformed to improve normality using the Box-Cox transformation method, as implemented in MASS v7.3.60.0.1 (Venables and Ripley 2013).

Disease prevalence was recorded as either present or absent and classified as white syndrome or black band disease, as defined in

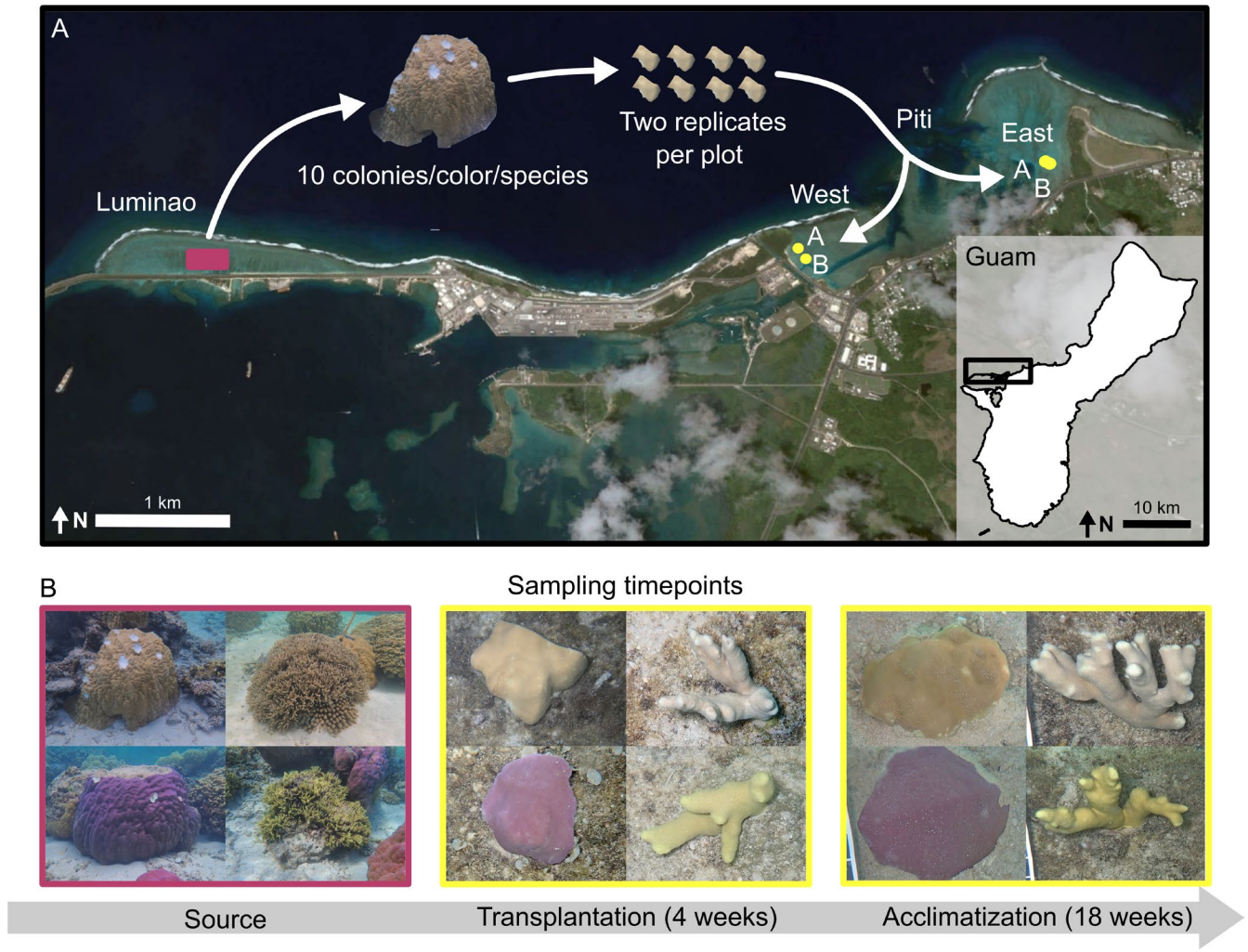

FIGURE 1 | (A) 10 sample colonies of *P. lobata* and *P. cylindrica* and their colour morphs (40 total), were sampled from Luminao reef flat (13° 27′ 58″ N, 144° 38′ 37″ E) off the island of Guam, Micronesia. Colonies were split into 8 fragments and then transplanted to 4 plots located in Piti Marine Preserve (East: 13°28′20″N 144°42′16″ E and West: 13°27′56″N 144°41′15″ E). (B) Tissue samples were taken at three timepoints (Source, Transplantation [4 weeks], and Acclimatisation [18 weeks]) to assess the changes in bacteria and Symbiodiniaceae communities, as well as, Symbiodiniaceae density.

Wills et al. (Willis et al. 2004). A final monitoring timepoint was collected to determine transplantation success 72 weeks (1 year and 3.5 months) later (September 27, 2022). Partial mortality was defined as areas of bare skeleton and binned from 0 to 6 (0: no bare skeleton, 1: 1%–10% bare skeleton, 2: 11%–25% bare skeleton, 3: 26%–50% bare skeleton, 4: 51%–75% bare skeleton, 5: 76%–99% bare skeleton, 6: dead). Statistical analyses for partial mortality are described in Section 2.7. Coral tissue samples were collected at three time points to assess clonal structure of source corals, assess Symbiodiniaceae density and diversity, and bacterial microbiome diversity patterns. Sampling time points included (i) baseline state of source colonies pre-transplantation (May 11, 2021; Figure 1B), (ii) approximately 4 weeks following transplantation to capture the response to transplantation (June 8, 2021; Figure 1B), and (iii) approximately 18 weeks (4 months) following transplantation to capture the acclimatised state of transplanted corals (September 30, 2021; Figure 1B). Samples were obtained by removing roughly 10 to 20 mm diameter fragments from the center of *P. lobata* colonies using a hammer and chisel, followed by immediate preservation in the field in liquid nitrogen. Similar-sized pieces of *P. cylindrica* branches were collected using wire cutters, taking samples that were approximately 2 cm from the tip to avoid new-growth tissues. Flash-frozen samples were stored at −80°C until further processing.

2.3 | Identifying Host Coral Genotypes

Total DNA was extracted from a small coral sample from all source coral colonies ($n = 40$) using the Qiagen DNeasy PowerSoil Pro Kit on a Qiacube extraction robot (Qiagen, Hilden, Germany) following the manufacturer's protocol. DNA extracts were prepared for 2b-RAD sequencing following Wang et al. (Wang et al. 2012). Technical replicate samples were prepared to assist with clone identification. A total of 37 samples were successfully barcoded and sequenced at Tufts University Core Facility (TUCF; Boston, MA) across four lanes of an Illumina HiSeq 2500 sequencer using high output v4 chemistry (Illumina, San Diego, CA) to generate 50 bp single-end sequence reads. Raw 2b-RAD reads were trimmed, deduplicated, and quality filtered

with the Fastx toolkit (http://hannonlab. cshl.edu/fastx_toolkit), retaining reads with Phred-scaled quality scores > 20 (−q 20 −p 100). Quality-filtered reads were first mapped to a concatenated genome of four Symbiodiniaceae genera—*Symbiodinium (*Aranda et al. 2016*), Breviolum* (Shoguchi et al. 2013), *Cladocopium* (Liu et al. 2018), and *Durusdinium (*Dougan et al. 2022*)*—using bowtie2 (Langmead and Salzberg 2012). Any reads that were mapped successfully with a minimum end-to-end alignment score of—22.2 or higher were removed so that remaining reads were free of symbiont contamination. The remaining reads were mapped to the *P. lobata* genome. Genotype calling was performed in ANGSD (Korneliussen et al. 2014), keeping loci present in at least 80% of individuals, a minimum mapping quality score of 20, a minimum quality score of 25, a strand bias $p > 0.05$, a heterozygosity bias > 0.05, a minor allele frequency (MAF) > 0.05, a SNP p-value of 1×10^{-5}, removing all triallelic sites, reads having multiple best hits, and lumped paralogs. Clones were detected using hierarchical clustering of samples based on pairwise identity by state (IBS) distances calculated in ANGSD. Technical replicates were used to identify the appropriate IBS distance cutoff in a combined dataset of *P. lobata* and *P. cylindrica*.

To identify the presence of cryptic coral lineages and assess whether the coral host genotype influenced patterns of bacterial or Symbiodiniaceae diversity, host genotype was identified using phylogenetic analyses. We also included massive *Porites* 2b-RAD-seq data from Starko et al. to assist with genotype assignment (Team RC 2013). Phylogenetic analyses were carried out using RAxML (Stamatakis 2014) under the GTRGAMMA model with 100 rapid bootstrap replicates. To root the phylogenetic tree, an outgroup of 2b-RAD-seq data from *Siderastrea siderea* was included in the RAxML analysis. To assign a genotype to each sample, ADMIXTURE (v. 1.3.0; 54) was used with an optimal K determined from RAxML analysis. If a sample had an ADMIXTURE assignment proportion > 0.75 for a single cluster, it was assigned to that genotype. Host genotype was used as a factor for PERMANOVA tests for differences in bacterial and Symbiodiniaceae communities (see Section 2.6).

2.4 | Symbiodiniaceae Cell Density

Tissue from all 480 coral samples (4 sites, 10 colonies, 4 morphospecies, and 3 timepoints) was airbrushed from the skeleton with 0.2 μm filtered seawater (FSW) and homogenised via vortexing and needle-shearing. One millilitre was transferred to 1.5 mL screw-top tubes, and the remaining tissue slurry was measured with a graduated cylinder. Samples were mixed for 5 s in a MiniBeadBeater Plus (BioSpec Products, Bartlesville OK) followed by centrifugation at 5000 rpm for 4 min. The supernatant was removed, and the pellet resuspended in 1 mL of FSW, followed by 5 s of homogenisation in the bead beater. Another round of centrifugation at 5000 rpm for 3 min was used to pellet Symbiodiniaceae cells. The supernatant was discarded, and Symbiodiniaceae were resuspended in 1 mL of SDS solution (8% sodium dodecyl sulfate (SDS), 7/8 deionised water (DI), 1/8 FSW) using 4 s of sample agitation in the bead beater. Then, two replicates of each sample were loaded into a microwell plate as a tenfold dilution in a 50/50 DI/FSW mixture. Two technical replicates of each well were processed with a Guava easyCyte flow-cytometer (Cytek Biosciences, Fremont CA) to count cells/mL based on red auto-fluorescence (Red-B 488 nm laser) and side scatter; the total Symbiodiniaceae cell count of the complete tissue slurry was obtained by scaling the concentration of cells determined by the flow cytometer to the total tissue slurry volume (Anthony, Lock, and Bentlage 2023).

To convert total Symbiodiniaceae cell counts associated with each coral fragment to Symbiodiniaceae densities in coral tissues (cells per cm^2), the surface area of the coral fragment was divided by the total cell count (for a detailed protocol see Anthony, Lock, Crisostomo, and Bentlage 2024). The surface area of coral skeletal fragments was determined using a 3D jewellery scanner (D3D-s, Vyshneve, Ukraine) to generate a point cloud accurate to 0.01 mm. Before scanning, fragments were mounted on staples and sprayed with SKD-S2 Aerosol (Magnaflux, Glenview, IL) to reduce refraction that may interfere with the scan. Point clouds of each fragment were individually imported into MeshLab v2020.04 to align point clouds and reconstruct the fragment's surface. Portions of the fragment which did not contain tissue were removed from the modelled fragment, and the remaining surface area was measured. In all comprehensive models, species had a consistently strong and significant effect ($p < 0.001$), while other factors showed weaker or inconsistent patterns across dual-species models. Given the limited clarity in the more comprehensive dataset, we fit species-specific repeated-measures ANOVAs, with individual ID included as a random effect, to better resolve the effects of colour, time, and location within each group. Residuals were assessed for normality via the Shapiro-Wilks test, then either log or cube transformed to meet the assumptions of normality. These tests were completed with base R v4.2.2 (Team RC 2013).

2.5 | Symbiodiniaceae and Bacterial Biodiversity

For metabarcoding, sequencing of all 480 samples for both 16S and ITS2 would have been cost prohibitive. Therefore, three colonies per morphospecies (purple *P. lobata*, brown *P. lobata*, brown *P. cylindrica*, yellow *P. cylindrica*) were selected for DNA extraction and metabarcoding. We selected corals that showed no signs of active disease lesions on the day of sampling to avoid extracting and sequencing possible disease-related bacterial assemblages. Source sampling consisted of 12 total colonies. The same colonies' transplanted counterparts were sampled at all four plots (West A, West B, East A, East B; Figure 1A) for a total of 48 samples per timepoint (Figure 1B). Although we discuss partial mortality and disease later, these observations were used to provide functional context, and we should note that additional characterisation of disease lesion microbiomes will be necessary to potentially link white syndrome observed by us to its causal agents, which have been explored in other publications (Sussman et al. 2008; Zhenyu et al. 2013).

Samples were randomly assigned to a PCR batch to reduce systematic biases and noise between sampling groups that possible PCR artefacts may have on downstream analyses. For each PCR, 30 ng of DNA were used to amplify the Internal Transcribed Spacer 2 (ITS2) by PCR (26 cycles of 95°C for 40 s, 59°C for 2 min, 72°C for 1 min, followed by a final elongation at 72°C for 7 min) using SYM_VAR_5.8S2 forward (5′-GAA TTG CAG AAC TCC

GTG AAC C-3′) and SYM_VAR_REV (5′-GGG ATC CAT ATG CTT AAG TTC AGC GGG T-3′) primers (Hume et al. 2018). The V4 hypervariable region of the 16S rRNA gene was amplified from each sample using universal bacterial primers 515F (Walters et al. 2016) and modified 806R (Apprill et al. 2015) (30 cycles of 95°C for 40 s, 58°C for 2 min, 72°C for 1 min, followed by a final elongation at 72°C for 5 min). The 30-μl PCR reactions included 3 μL of template DNA, PCR grade water, 1× ExTaq buffer (Takara Bio, San Jose, CA), 2.5 mM dNTPs, 10 μM forward and 10 μM reverse primers, and 0.75 U ExTaq DNA Polymerase (Takara Bio, San Jose, CA). After amplification of the ITS2/16S region, each sample was barcoded with a unique Illumina index primer (5 cycles of 95°C for 40 s, 59°C for 2 min, 72°C for 1 min, followed by a final elongation at 72°C for 7 min). PCR products (ITS2 and 16S) were purified after amplification using a GeneJet PCR purification kit following the manufacturer's protocol (ThermoFisher Scientific, Rockford, IL, USA). Successfully amplified and barcoded ITS2 samples were randomly pooled into batches of 96 samples with 4 samples carried over onto the next sequencing run. A PERMANOVA between samples from each sequencing run determined there were no significant differences and the duplicates were removed from further analysis. Pooled samples were run on a 2% agarose gel with SYBR green dye, visualised on a blue light box, and size selected by excising the target band from the gel, followed by incubation of gel fragments in 200 μL ultrapure UV-sterilised and filtered (0.22 μm) water at 4°C overnight. The pooled and size-selected sequencing libraries were purified using a GeneJet PCR purification kit. Pooled products were sequenced in three runs (one for 16S and two for ITS2) on an Illumina MiSeq by CDgenomics (New York City NY) using v3 (2 × 300 bp) reagents. Sequence data were deposited in NCBI GenBank's short read archive (16S: SRR33748254—SRR33748361; ITS2: SRR33748254—SRR33748361), accessible through BioProject PRJNA1211696.

2.6 | Bioinformatics and Statistical Analyses of Microbial Community Data

For both Symbiodiniaceae and bacterial sequences, primers were removed using CutAdapt (Version 4.0; Martin 2011). Symbiodiniaceae ITS2 data were processed through SymPortal (Hume et al. 2019) to generate relative abundances of Symbiodiniaceae clade/sub-clade defining intragenomic variants (DIVs) and ITS2 type profiles. For bacterial diversity, the RStudio package DADA2 (Callahan et al. 2016) was used to remove primer sequences, truncate reads, calculate error rates, de-duplicate reads, and infer amplicon sequence variants (ASVs) after merging paired reads and removal of chimeras. Non-chimeric ASVs were assigned a taxonomy using the Silva v138 database (Quast et al. 2012) using a naive Bayesian classifier with a minimum bootstrap confidence of 50. The phyloseq package (McMurdie and Holmes 2013) was used to remove ASVs whose taxonomy matched 'Mitochondria', 'Chloroplast', or 'Eukaryota' MCMC.OTU was used to remove ASVs representing < 0.1% of count data and to identify putative outlier samples (total count less than 2.5 standard deviations below the mean). Final graphics were produced using ggplot2 (v3.3.5). A PERMANOVA implemented via the adonis2 function in the vegan R package (version 2.3-5; Dixon 2003) identified differences between Symbiodiniaceae/bacterial assemblages across coral species or within coral species for colour morphology, site, plot, and time using colony as a random effect. Bray–Curtis dissimilarity distances were calculated for each species for both the Symbiodiniaceae and bacterial communities, which were visualised in NMDS plots using ggplot2. Two-way ANOVAs were used to test for significant differences in alpha diversity of bacteria and Symbiodiniaceae with colony as a random effect.

Bacteria belonging to *Endozoicomonadaceae* ASVs were identified to the genus level using a phylogenetic analysis that contained publicly available 16S sequences representing the diversity of the family. Sequences were aligned using MUSCLE (version 3.8.1551; Edgar 2004), followed by removal of ambiguous regions of the alignment using Gblocks (version 0.91b; Castresana 2000) allowing for smaller final blocks, gap positions within final blocks, and less strict flanking positions, as implemented in SeaView (version 4.7; Gouy et al. 2010). PhyML (version 3.3.3; Guindon and Gascuel 2003) was used to infer the maximum likelihood phylogeny of *Endozoicomonadaceae* after identifying the nucleotide substitution model that best fit the data under the Akaike Information Criterion (AIC) using jModelTest (version 2.1.10; Darriba et al. 2012). Robustness of the phylogeny was inferred using 1000 non-parametric bootstrap replicates.

2.7 | Statistical Analyses for Post-Transplantation Monitoring

Partial mortality of all corals 72 weeks after transplantation was evaluated using an ordinal logistic regression model. The response variable, partial mortality, was analysed as an ordered factor given that it was categorised into seven ordinal levels (0–6; see Section 2.2) representing increasing degrees of partial mortality. The model was fit using the cumulative link mixed model (CLMM) framework from the ordinal package (v2023.12-4; Christensen and Christensen 2015) in R (v4.2.2.) Fixed effects included species, colour morph, and plot, while a random intercept for colony ID was included to account for repeated measures or clustering within individuals. After fitting the model, the 'summary' function was used to extract coefficient estimates, standard errors, and significance tests for the fixed effects. To evaluate the significance of each predictor, a likelihood ratio test (LRT) was conducted using the 'drop1' function, which sequentially removed terms from the model and compared nested models via chi-squared tests. Afterwards, to evaluate specific pairwise distributions of interest, Wilcoxon rank-sum tests were employed with the exact distribution method, ensuring robust inference even with small sample sizes or ties in the data, as implemented in the coin package (v1.4.3; Hothorn et al. 2008).

Based on 2b-RAD-seq (coral genotype), ITS2 (Symbiodiniaceae community), and 16S sequencing data (bacterial community), corals were assigned additional characteristics and then evaluated within the context of their partial mortality 72 weeks after transplantation. *P. lobata* colonies were assigned 1 of 5 genotypes, as determined by ADMIXTURE analysis (c.f. Section 2.3), to evaluate whether genotype influenced transplantation and acclimatisation success. Again, the CLMM framework was used

TABLE 1 | The results of Adonis test of *Symbiodiniaceae* DIVs and bacterial ASVs (Figure 5) on different factorial levels.

		Porites lobata		*Porites cylindrica*	
	Df	**Symbiodiniaceae Pr(>F)**	**Bacteria Pr(>F)**	**Symbiodiniaceae Pr(>F)**	**Bacteria Pr(>F)**
Colour	1	0.009**	0.001***	0.0007***	0.392
Time	2	0.572	0.046*	0.125	0.001***
Plot	3	0.248	0.021*	0.116	0.007**
Site (East vs West)	1	0.298	0.395	0.306	0.352
Time:Plot	3	0.054	0.441	0.281	0.001***
Coral host genotype *(P. lobata* only)	4	0.789	0.9201		

Note: Only *Porites lobata* showed multiple genotypic lineages in 2b-RAD analysis and were used as a factor for Adonis tests on Symbiodiniaceae and bacterial diversity patterns (see Section 3.5). Site (East vs. West) was insignificant in all tests and removed as a factor from statistical models. * indicates p-value <0.05, ** indicates p-value <0.01, indicates p-value <0.001.

to evaluate the relationship between genotype and partial mortality with genotype (Knowlton et al. 2010; Cinner 2014; Hughes et al. 2017; Maor-Landaw and Levy 2016; Anthony, Lock, et al. 2023) as a fixed effect and colony ID as a random intercept.

Colonies with ITS2 data were categorised as 'yes' or 'no' for ITS2 type profile shifts at both 4 weeks and 18 weeks compared to their source timepoint and correlated to the partial mortality that was observed for that colony. Similarly, the partial mortality of colonies at 72 weeks with 16S community data was plotted against the relative abundance of *Endozoicomonadaceae* at both 4 weeks and 18 weeks after transplantation. A generalised linear mixed-effects model (GLMM) fit by maximum likelihood with a Poisson distribution and a log-link function was implemented using the glmer function from the lme4 package in R (version 1.1.35.3; Bates et al. 2015). The fixed effects included the categorical predictors ITS2 shifts at 4 weeks, ITS2 shifts at 18 weeks, *Endozoicomonadaceae* relative abundance at 4 weeks, and *Endozoicomonadaceae* relative abundance at 18 weeks. Individual identity (ID) was included as a random intercept. This process was then repeated for each species separately to evaluate species-specific effects. Colour phenotypes were omitted from models based on previous results that colour did not influence mortality.

3 | Results

3.1 | Environmental Characterisation

Water temperature was similar between east and west common garden plots, with average temperatures about 0.25°C higher in the eastern plots compared to western plots (Figure S2A). The temperature difference was most apparent during the hottest months of the year (June–August; Figure S2A). Temperature at the gardens on May 15, 2021 (4 days after transplantation) was 29.4°C with a range of ~1.5°C. Towards the end of the month, mean temperatures increased slightly to between ~29.5 and 30°C, with maximums reaching close to 33°C. On the day of the first sampling, water temperature was 29.7°C at the East site and 29.6°C at the West site on average, with maximums of 31.8°C and 30.5°C respectively. The temperature stabilised by the following sampling timepoint on September 30 with the daily average at both sites being 29.8°C and the maximum temperature being 30.2°C in the West and 30.3°C in the East on that day. The difference in water temperatures between the source location (Luminao) and the transplantation plots was less than 0.25°C (Figure S2A). Light levels at different sites seemed similar based on a limited 7-day dataset (Figure S2B), although inconclusive due to limited viable measurements before biofouling. Water depth varied by about 20 cm on average between the east and west plots (Figure S2C). No differences in orthophosphate, nitrite, and nitrate between sites were observed (< 0.010 mg/L for both sites).

3.2 | Coral Host Genotyping

Analysis of 2b-RAD data revealed two clonal colonies in *P. lobata* (B1 and B2; Figure S3) and three in *P. cylindrica* (B1, B2, and B9; Figure S3). In order to capture the microbial dynamics of the overall *Porites lobata* population instead of a specific genotype, clonal replicates were removed from Symbiodiniaceae density and microbiome (Symbiodiniaceae and bacteria) diversity analyses. Although there were few clones in *P. cylindrica*, admixture analysis assigned all colonies to the same genotype. Admixture genotype assignment identified five genotypes for *P. lobata* (Figure S3). Genotype assignment did not separate the colour morphologies of *P. lobata*; several genotypes contained both brown and purple colonies (see Table S1 for the assignments for each colony and colour morphology). Genotype was used as a factor in statistical analyses for Symbiodiniaceae and bacterial diversity of *P. lobata* to determine whether coral host identity had an influence on microbial diversity patterns (Table 1); genotype was not a factor in statistical analyses of *P. cylindrica* due to the observed lack of genetic diversity in this species.

3.3 | Coral Bleaching and Symbiodiniaceae Cell Density

Due to the nature of coral colour morphs, coral colour intensity was only considered within species-specific colour morphs to focus on spatio-temporal effects that may represent stress. All

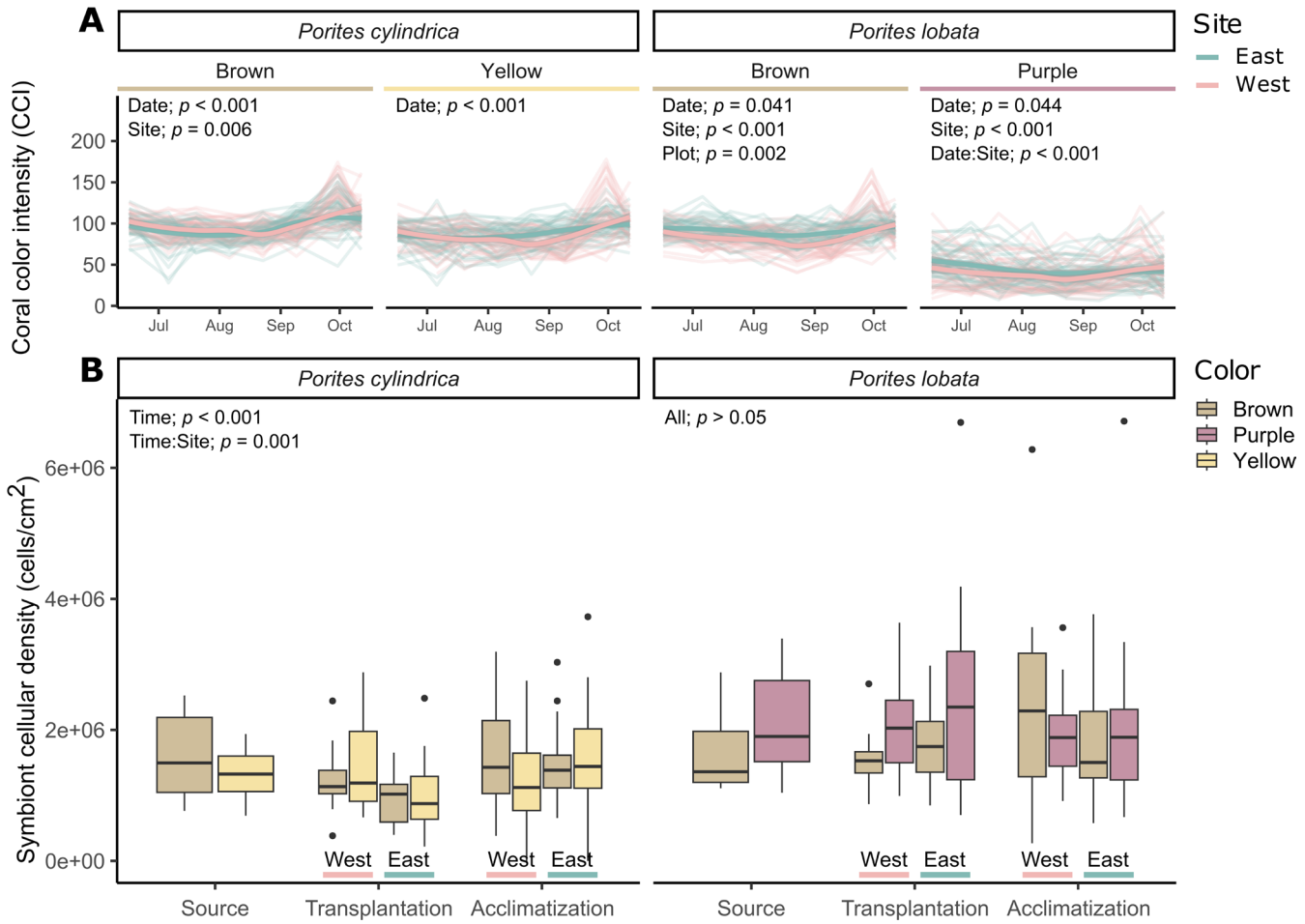

FIGURE 2 | (A) Grayscale calibrated CCI of all corals (Figure 1) through time to visualise the repeated monitoring of *P. cylindrica, P. lobata* and their colour morphs (brown, yellow, and purple) at eight evenly distributed sampling timepoints between June 8th, 2021 and October 12th, 2021. For CCI, 0 represents black, and 199 represents white. (B) Symbiodiniaceae cell density in *P. cylindrica* and *P. lobata* and their colour morphs at the three sampling timepoints: Source (May 12th, 2021), Transplantation (4 weeks later; June 8th, 2021), and Acclimatisation (18 weeks later; September 30th, 2021). *p*-values represent the significant results of the associated graph's repeated-measures ANOVA, which evaluated time, location, and colour as possible factors influencing data variation. Colour was tested separately for CCI to avoid bias caused by the base colour morphology (e.g., purple is darker than brown).

four groups darkened slightly through August and then paled slightly through September (brown *P. cylindrica*: $p < 0.001$; yellow *P. cylindrica*: $p < 0.001$; brown *P. lobata*: $p = 0.041$; purple *P. lobata*: $p = 0.044$; Figure 2A). Spatial effects were more variable, though generally corals were marginally darker in the west site (brown *P. cylindrica:* $p = 0.006$; brown *P. lobata*: $p < 0.001$; purple *P. lobata*: $p = 0.002$). Brown *P. lobata* had only a slight plot-specific interaction ($p = 0.002$), but no other spatial effects. Despite this significant differentiation between plots, variance within plots was extremely high, and within the context of data from cohabitating *A. pulchra* (Anthony, Lock, Pérez-Rosales, et al. 2024), temporal dynamics were mild and no mass coral bleaching occurred.

In *P. cylindrica*, symbiont cell density varied significantly over time ($p < 0.001$) and showed a clear spatio-temporal interaction ($p = 0.001$), suggesting location-dependent temporal dynamics. Indeed, Symbiodiniaceae densities decreased in both yellow and brown *P. cylindrica* by 28%, on average, with corals in the East garden having a more pronounced effect following transplantation (Figure 2B). Both locations recovered to baseline densities after 18 weeks (Acclimatisation; Figure 2B). In contrast, *P. lobata* was spatio-temporally stable. Neither species model indicated a colour-specific effect on cell density ($p > 0.05$).

3.4 | Symbiodiniaceae Species-Specific Patterns

Symbiodiniaceae communities for both *P. cylindrica* and *P. lobata* were dominated by ITS2 profiles belonging to *Cladocopium* C15 containing several inferred C15 types in almost all samples (Figure 3A). Symbiodiniaceae communities in *P. cylindrica* at the source site were all dominated by the same ITS2 profile (C15.C15by.C15er.C15kh; Figure 3A), thus explaining the tight cluster in the *P. cylindrica* NMDS plot (Figure 4B). All changes in *P. cylindrica* Symbiodiniaceae diversity indices (Figure 4) were driven by rearranged C15 types in nine colonies (Figure 3). In the brown *P. cylindrica* colour morph, three colonies changed type profiles after transplantation, but all reverted to source colony profiles by the acclimatisation timepoint of 18 weeks following transplantation. Yellow colonies demonstrated the opposite

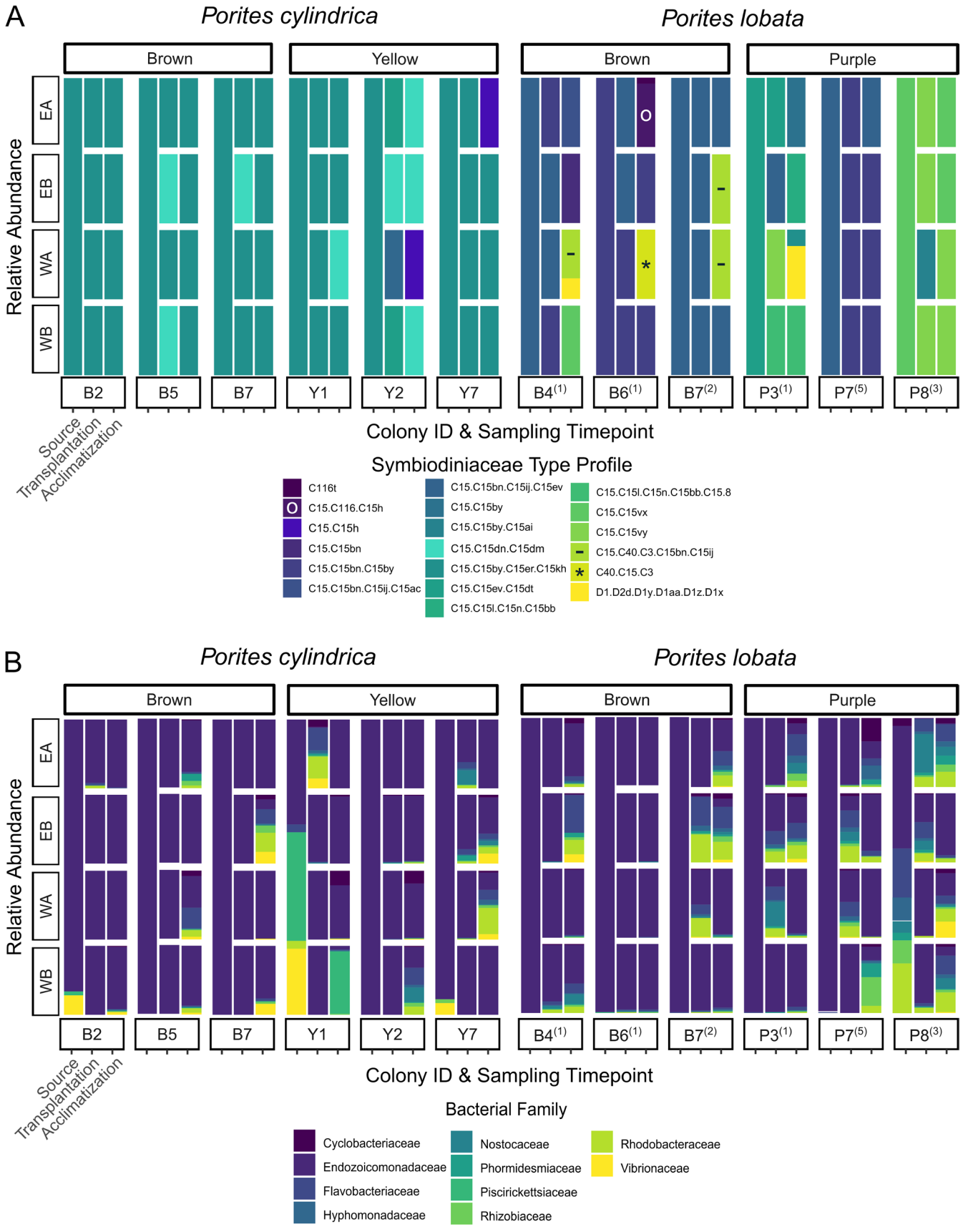

FIGURE 3 | Legend on next page.

FIGURE 3 | (A) Relative abundances of Symbiodiniaceae type profile in *P. cylindrica* and *P. lobata* and their colour morphs (brown, yellow, and purple) at the three sampling timepoints: Source (May 12th, 2021), Transplantation (4 weeks later; June 8th, 2021), and Acclimatisation (18 weeks later; September 30th, 2021). A single sample (Colony IDs on the x-axis; i.e., "B2") was collected for each colony at the source and split into four replicate colonies for each of the replicate plots: Piti West B (WB), West A (WA), East B (EB), & East A (EA). The genotype that each *P. lobata* colony belongs to is listed in parentheses after the colony ID (i.e., Knowlton et al. 2010; Figure S3; see Section 3.2). *Porites cylindrica* colonies were all from the same lineage. See Table S3 for a complete list of relative abundances of type profiles. (B) Relative abundances of bacterial families in both coral species and their colour morphs at the three sampling timepoints and four transplantation plots.

pattern with one yellow *P. cylindrica* colony changing to three different C15-based ITS2 profiles across all sites following transplantation that persisted through acclimatisation 18 weeks later (Figure 3A). Two additional colonies only had different C15-based ITS2 profiles after acclimatisation, with no sign of shifts immediately following transplantation.

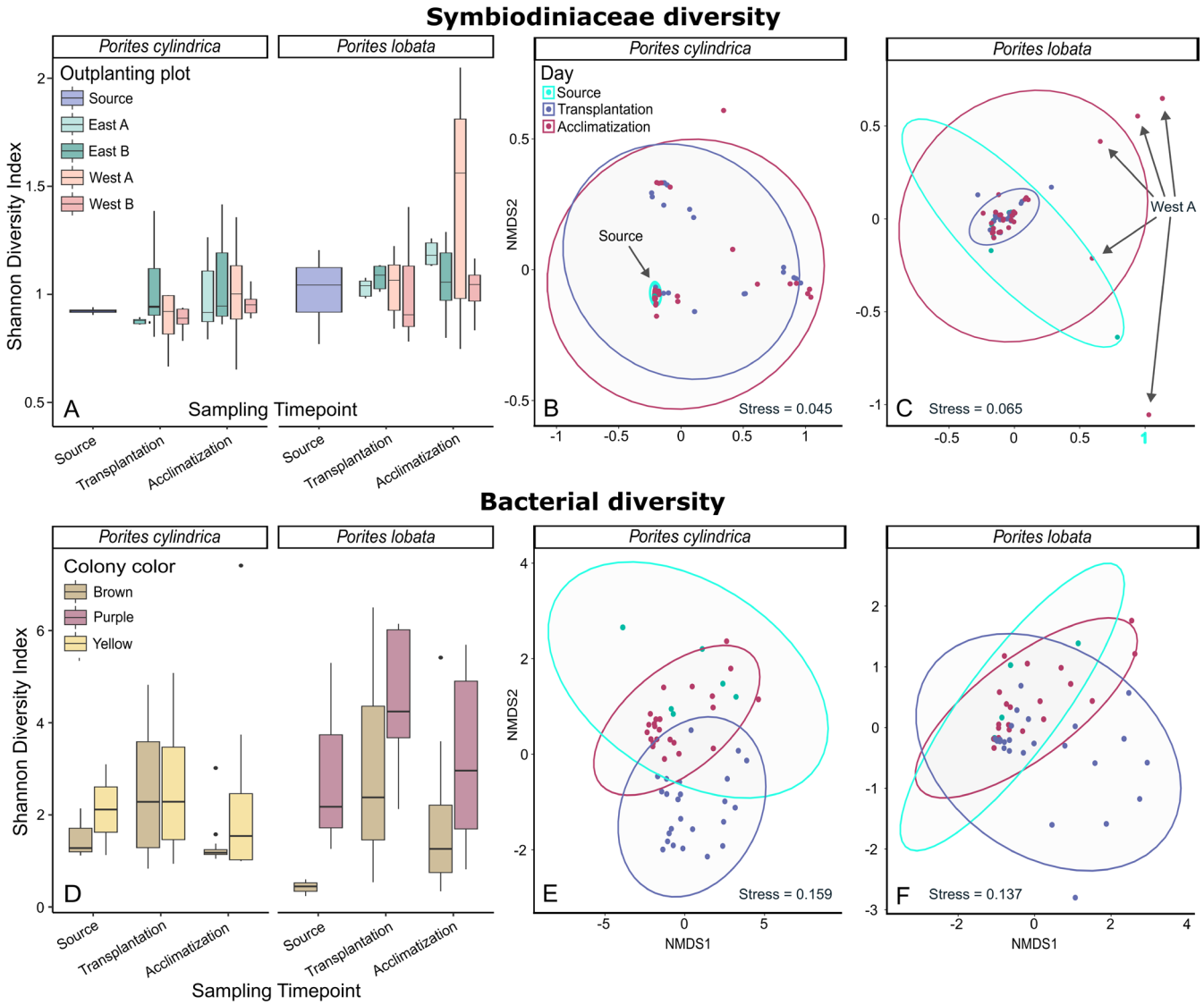

FIGURE 4 | Monitoring data to evaluate transplantation success of transplanted *P. cylindrica* and *P. lobata*. (A) Final partial mortality scores of each species and its colour morphs 72-weeks after transplantation (September 27th, 2022). Full partial mortality data is visualised in Figure S5. (B) Quantity of corals with active disease lesions within the first 18 weeks of monitoring. (C) Partial mortality of *P. lobata* 72 weeks after transplantation based on host genotype (Figure S3). The numbers below each boxplot indicate the number of source colonies with this genotype and number of fragments with data at the 72-week timepoint. *p*-value was derived from CLMMs after LRT analyses. (D–G) Partial mortality of coral colonies that were sequenced for ITS2 and 16S metabarcoding 72 weeks after transplantation. Numbers indicate the number of colonies observed at 72 weeks. (D, E) Symbiodiniaceae shift was recorded as 'yes' if colonies at 4 or 18 weeks had a different ITS2 type profile than their source colonies (Figure 3A). (E) Relative abundance of *Endozoicomonadaceae* values were derived from sequencing data collected at 4 or 18 weeks after transplantation. (A, B) Colours of boxplots indicate colour morphologies of *P. cylindrica* and *P. lobata*. (A, C–G) Partial mortality was scored semi-quantitatively from 0 to 6 with 0 being total healthy and 6 being dead. Read lines indicate the threshold for completely dead colonies. (D–G) *p*-values were derived from species-specific GLMERs.

TABLE 2 | The results of 2-way ANOVA tests of Shannon diversity index (Figure 4) on different factorial levels.

		Porites lobata		*Porites cylindrica*	
	Df	**Symbiodiniaceae Pr(>F)**	**Bacteria Pr(>F)**	**Symbiodiniaceae Pr(>F)**	**Bacteria Pr(>F)**
Colour	1	0.108	0.007**	0.011*	0.098
Time	2	0.207	0.043*	0.425	0.092
Plot	3	0.138	0.001**	0.192	0.145
Site (East vs West)	1	0.396	0.156	0.353	0.945
Time:Plot	3	0.179	0.835	0.988	0.712
Coral host genotype (*P. lobata* only)	4	0.443	0.391		

Note: Only *Porites lobata* showed multiple genotypic lineages in 2b-RAD analysis and was used as a factor for statistical tests on Symbiodiniaceae and bacterial diversity patterns (see Section 3.5). Site (East vs. West) was insignificant in all tests and removed as a factor from statistical models. * indicates p-value <0.05, ** indicates p-value <0.01.

All *P. lobata* sampled were dominated by *Cladocopium* C15 ITS2 type profiles at initial sampling from the source colonies, but harboured a more diverse set of C15-based ITS2 type profiles than *P. cylindrica* ($p=0.0001$), with four different type profiles in source colonies: (1) C15-C15by-C15er-C15kh, (2) C15-C15bn-C15by, (3) C15-C15bn-C15ij-C15ev, (4) C15-C15ev-C15d. Many of these colonies (11/15) shifted to different *Cladocopium* C15 types, whereas four colonies shifted to substantially different ITS2 profiles, dominated by *Cladocopium* C116 or C40, or even *Durusdinium* D1 (Figure 3A). Specifically, the only colonies that shifted to C40 or D1 ITS2 profiles were the *P. lobata* colonies in plot West A, which explains the separation of colonies in this plot in the acclimatisation NMDS (Figure 4C).

3.5 | Bacterial Community Composition

16S sequencing produced an average of 57,433 reads per sample after DADA2 filtering for 110 samples in total. Three hundred thirty five ASVs had a cumulative abundance of more than 1000 reads across all samples and were included in further analysis. Most colonies (10/12) were dominated (>90% relative abundance) by *Endozoicomonadaceae* at the source site (Figure 3B). Other major contributors to the relative abundance of the bacterial communities of these coral colonies were *Vibrionaceae, Piscirickettsiaceae, Rhizobiaceae, Rhodobacteraceae*, and *Nostocaceae* (Figure 3B). Almost all *Endozoicomonadaceae* ASVs (>99.9%; Table S2) were most closely related to *Parendozoicomonas* species (Figure S4). For two ASVs that fell within *Endozoicomonas*, the short ~260 bp ASV sequences were identical with *Endozoicomonas acroporae* and a strain of *Endozoicomonas* recently isolated associated from *Acropora pulchra* in Guam (de la Vega et al. 2023). *Endozoicomonas* ASVs were found in extremely low abundance (<1800 reads across all samples; Table S2) while the majority of ASVs assigned to *Endozoicomonadaceae* belonged to *Parendozoicomonas*. Considering the dominance of *Endozoicomonadaceae* in our analysis, we relied on phylogenetic analysis to discern among bacterial genera in this family. In general, it is important to note that ASVs identified in Table S2 cannot be interpreted as synonymous with bacterial species or strains without further in-depth phylogeny-based analyses. Consequently, our bacterial microbiome diversity analyses were based on family-level taxonomic assignments, effectively summing read counts across ASVs assigned to the same family to reduce the noise associated with potentially spurious lower-level taxonomic assignments.

Bacterial microbiome community shifts were apparent for both coral species after transplantation and acclimatisation (Figure 3B), but these shifts appeared most pronounced in *P. lobata*, which may in part reflect the greater host genotype diversity represented in this species (Figure S3). However, genotype was not a significant factor explaining variation in *Porites lobata* microbial communities (Symbiodiniaceae or bacteria; Tables 1 and 2). *Vibrionaceae* appeared in half (3/6) of the source colony fragments of *P. cylindrica* (Figure 3B). *Vibrionaceae* taxa are often associated with disease, but no disease was observed during initial sampling or following transplantation of these specific colonies. *Vibrionaceae* abundance did not follow predictable patterns through time. Many fragments that initially harboured *Vibrionaceae* showed none at subsequent timepoints and, conversely, *Vibrionaceae* ASVs appeared in some samples that did not harbour these bacterial taxa during initial sampling at the source site. Irrespective of the starting composition of bacterial microbiomes, most *P. cylindrica* fragments (42/46) remained, or in the case of one yellow *P. cylindrica* (Y1; Figure 3B) became dominated by *Endozoicomonadaceae* (*Parendozoicomonas*) following transplantation and acclimatisation. While *Vibrionaceae* were not detected in any appreciable number in the source colonies of *P. lobata*, *Vibrionaceae* were apparent in some samples collected after transplantation and acclimatisation (Figure 3A).

3.6 | Microbiome Diversity Dynamics

Porites lobata colonies harboured more diverse Symbiodiniaceae communities than *P. cylindrica* across the entire study (Adonis test $p=0.0001$; Figure 4A). Both *Porites* spp. harboured significantly different Symbiodiniaceae communities between colour morphs (Table 1). Alpha diversity (Shannon index) was relatively stable across the three timepoints in *P. cylindrica* ($p=0.125$) and in *P. lobata* ($p=0.572$; Figure 4A). However, beta diversity revealed that the microbiome of *P. cylindrica* exhibited a more variable response to transplantation and acclimatisation

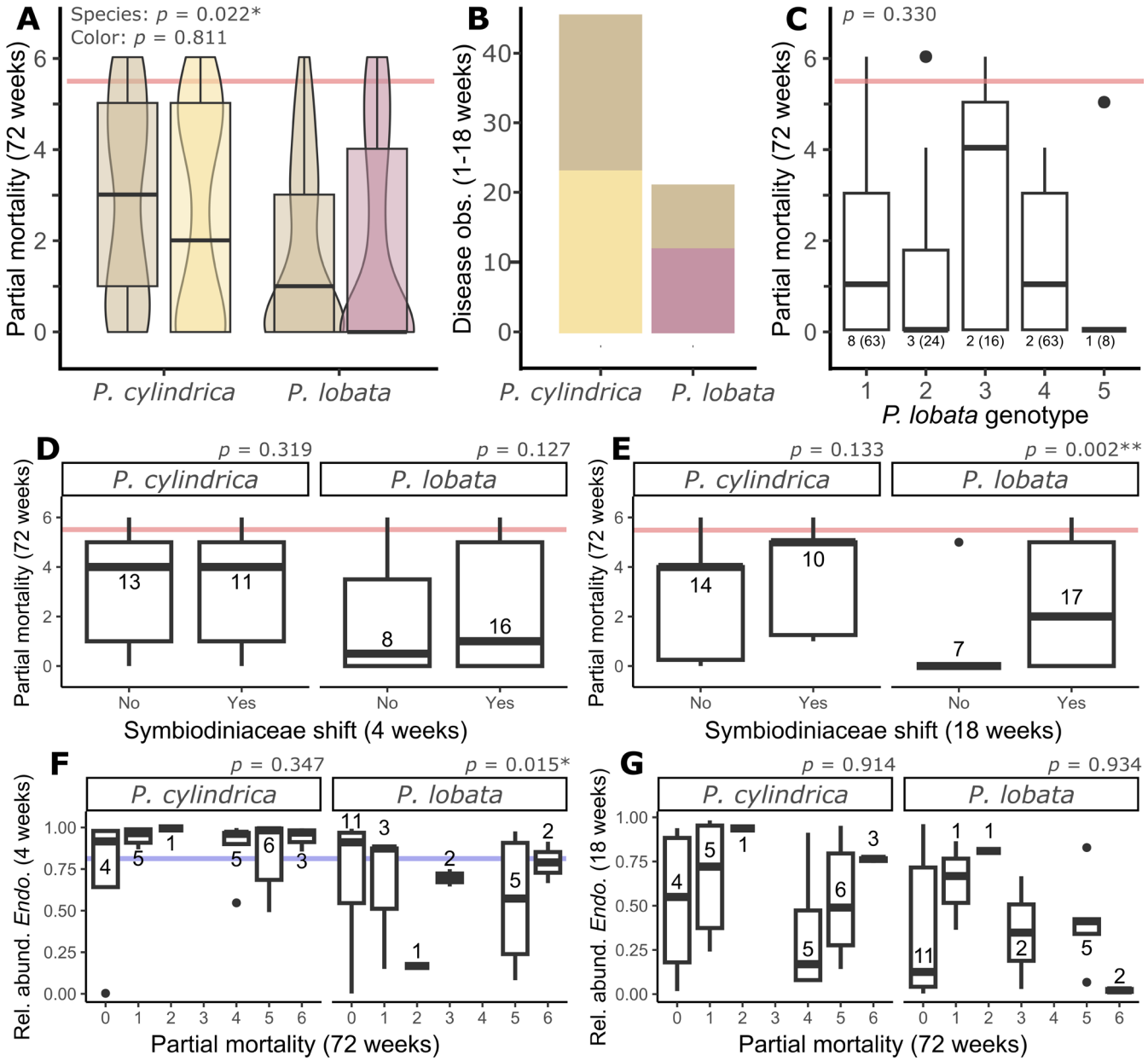

FIGURE 5 | (A) Shannon diversity index (alpha diversity) of Symbiodiniaceae DIVs for *P. cylindrica* and *P. lobata* and their colour morphs at the three sampling timepoints: Source (May 12th, 2021), Transplantation (June 8th, 2021), and Acclimatisation (September 30th, 2021). (B, C) NMDS plot of Bray–Curtis Dissimilarity Distances (beta diversity) from Symbiodiniaceae DIVs with ellipses representing the three sampling timepoints for (B) *P. cylindrica* and (C) *P. lobata*. Several outlier points from plot West A are highlighted, where significant shifts in symbiont community occurred. (D) Shannon diversity of bacterial ASVs for *P. cylindrica* and *P. lobata* and their colour morphs at the three sampling timepoints. (E, F) NMDS plot of Bray–Curtis Dissimilarity Distances (beta diversity) from bacterial ASVs with ellipses representing the three sampling timepoints for (E) *P. cylindrica* and (F) *P. lobata*.

compared to *P. lobata* (Figure 4B,C). This was reflected in the homogeneous beta diversity of its source colonies and the increased variance in beta diversity following transplantation (Figure 4B). In contrast, the beta diversity of *P. lobata* microbiomes showed a more consistent response to transplantation and acclimatisation, except for plot West A (Figure 4C).

For bacteria, Shannon diversity index ($p = 0.046$) and relative abundances ($p = 0.001$) revealed significantly higher bacterial diversity in *P. lobata* compared to *P. cylindrica* (Figure 4D). Time, plot, and colour were all significantly different for Shannon and observed diversity in *Porites lobata* (Tables 1 and 2), whereas only time and plot were significant for observed diversity in *Porites cylindrica* (Table 1). *P. lobata* colour morphs harboured significantly different bacterial communities (Adonis $p = 0.001$; Figure 4D), whereas there was no significant difference in bacterial microbiome composition between *P. cylindrica* colour morphs (Figure 4D).

3.7 | Ecological Monitoring After Transplantation

As far as visible signs of transplantation success, 4 weeks after transplantation, only 5.6% (18/320) of colonies had any partial

mortality; all were categorised as 1 (1%–10% bare skeleton) or 2 (11%–25%). All 302 other colonies lacked exposed skeleton. Eighteen weeks after transplantation, 20.6% (66/320) of transplanted colonies showed some partial mortality. Only two colonies had died, which were not used for microbiome analysis. *P. cylindrica* had significantly lower mortality than *P. lobata* at this point (Wilcoxon, $Z = -3.787$ $p < 0.001$), as 28.8% (19/66) of colonies with mortality were *P. cylindrica*, with the other 71.2% of partial mortality observed in *P. lobata*. Upon returning to the plot 72 weeks after transplantation, this pattern flipped (LRT, $\chi^2 = 5.23$, $p = 0.022$; Wilcoxon, $Z = 4.266$, $p < 0.001$). Seventy two weeks after transplantation, 60.8% (194/319; one colony was missing) of all colonies had some partial mortality, 59.3% (115/194) of which were *P. cylindrica* (Figure 5A). Of all remaining *P. cylindrica* colonies, 46.9% (75/160) were estimated at > 50% partial mortality, compared to only 25.2% (40/159) of *P. lobata* colonies (Figure 5A). *P. cylindrica* performed substantially worse in the West plots than the East plots (Figure S5), which likely caused the statistical significance of location as a factor in our CLMMs (LRM, $\chi^2 = 21.75$, $p < 0.001$). Colour showed no sign of influencing partial mortality (LRT, $\chi^2 = 0.42$, $p = 0.811$). Upon returning to the plots in 2024 (3 years after transplantation), nearly all *P. cylindrica* had died in the West plots, while many *P. lobata* remained across both plots, although mortality was not quantified. Partial mortality of corals sampled for microbiome sequencing ($n = 48$ across species and colour morphs) was similar to the total population of corals outplanted and monitored across common garden plots ($n = 320$).

Partial mortality of corals at 72 weeks after initial transplantation reflected general disease prevalence of colonies (by species and colour morph) within the first 18 weeks. Over twice the observations of active disease lesions on *P. cylindrica* compared to *P. lobata* colonies (Figure 5B). In total, 98% (65/66) disease observations for both species were classified as 'white syndrome' (Willis et al. 2004). Given the fluctuating dynamics of disease lesions, partial mortality was used to evaluate transplantation and acclimatisation success from this point forward. Further, we only discuss partial mortality for colonies monitored 72 weeks after transplantation given the extremely low mortality directly following transplantation (Figure S5) and the avoidance of unhealthy colonies for 16S and ITS2 sequencing, as it is the best data to relate genotypic data to transplantation success.

Our initial model indicated that shifts in Symbiodiniaceae community 18 weeks after transplantation predicted increased partial mortality 72 weeks after transplantation (GLMM, $Z = 2.521$, $p = 0.012$; Figure 5D). Species-specific models showed that this result was driven by *P. lobata* (GLMM, $Z = 3.128$, $p = 0.002$), rather than *P. cylindrica* (GLMM, $Z = 1.501$, $p = 0.133$). Colonies that maintained their ITS2 type profile throughout the first 18 weeks showed the least amount of partial mortality with 85.7% (6/7) remaining completely healthy without any signs of partial mortality. Interestingly, increased partial mortality was correlated with shifts between inferred subclades among C15 ITS2 type (e.g., C15-C15l-C15n-C15bb type profile shift to C15-C15by type profile). Of the six *P. lobata* colonies that acquired non-C15 ITS2 types (Cladocopium C40, C116, and Durusdinium D1; Figure 3A), all were still alive 72 weeks after transplantation. Of these, 83.3% (5/6) had less than 50% partial mortality (PM score ≤ 3).

The *P. lobata* exclusive model also revealed a relationship between a lower relative *Endozoicomonadaceae* 4 weeks after transplantation and partial mortality at 72 weeks. Specifically, colonies with less *Endozoicomonadaceae* had higher mortality. Within the same model, correlation of fixed effects suggested a relationship between this lower abundance of *Endozoicomonadaceae* at 4 weeks and an ITS2 switch at 18 weeks (GLMM, $\rho = -0.621$).

Models indicated that partial mortality was neither a product of early Symbiodiniaceae community shifts (e.g., GLMER, $Z = -1.112$ $p = 0.266$; Figure 5D), nor the relative abundance of *Endozoicomonadaceae* 18 weeks after transplantation (e.g., GLMER, $Z = -0.327$, $p = 0.743$; Figure 5G). Genotype was not a significant contributor to partial mortality (LRT, $\chi^2 = 4.604$, $p = 0.330$), indicating that observed patterns of partial mortality may be attributed to source colony identity rather than the genotype (Figure 5C).

4 | Discussion

4.1 | Overview

This study describes the transplantation and initial acclimatisation dynamics of the Symbiodiniaceae and bacterial microbiome communities associated with two dominant reef-building corals, *P. cylindrica* and *P. lobata*. Symbiodiniaceae and bacterial communities displayed distinct responses to transplantation that differed between these congeneric coral species. Both Symbiodiniaceae and bacterial communities associated with *P. lobata* responded to transplantation more dramatically than those in *P. cylindrica* (Figures 3 and 4). Notably, we observed shifts in both communities, typically towards a diversified community (Figure 4), such as the introduction of new ITS2 type profiles (Figure 3A) or a transition away from *Endozoicomonadaceae*-dominated bacterial communities (Figure 3B). However, within these transitions, there was high variation in the timing and magnitude of bacterial community shifts observed. Some corals maintained similar bacterial communities through transplantation stress (4 weeks) and into site acclimatisation (18 weeks), while other colonies diversified after transplantation before converging upon source communities (Figure 3). Monitoring of partial mortality and disease showed clear species-specific differences in fitness, while colour morphology had no influence. Incorporating this monitoring data with metabarcoding sequencing revealed additional insights into how microbiome shifts potentially affect the overall coral holobiont, with a particular focus on the ITS2 community.

4.2 | *Porites* Affinity for *Cladocopium* C15

Porites spp. acquire their symbionts primarily through vertical transmission (LaJeunesse et al. 2004), which may lead to *Porites'* strong specificity for *Cladocopium* C15 (Putnam et al. 2012; Claar et al. 2020; Cunning et al. 2017; Fifer et al. 2022). Consistent with this, nearly all sequenced colonies in our study contained C15-dominated Symbiodiniaceae assemblages. However, we observed shifts in *Cladocopium* C15 types in both *P. cylindrica* and *P. lobata* after transplantation (Figure 3A). Notably, *P. cylindrica* exhibited less variable ITS2 type profiles compared to

P. lobata, with shifts in all colonies restricted to *Cladocopium* C15 subtypes (Figure 3). Among *P. cylindrica*, shifts occurred more frequently in yellow colour morphs than in brown colour morphs (Tables 1 and 2). These observations suggest a degree of plasticity within the tightly coevolved symbiotic relationship, potentially allowing acclimatisation to new environments (Cunning et al. 2015; Hauff et al. 2016).

Differences in Symbiodiniaceae types have been linked to variability of coral stress tolerance (Berkelmans and Van Oppen 2006; Hoadley et al. 2021; Stat et al. 2008; Xiao et al. 2022; Díaz-Almeyda et al. 2017). Thus, understanding the traits of Symbiodiniaceae and symbiont shifts in response to transplantation is critical for coral reef restoration efforts. Functional differences have been documented both between major Symbiodiniaceae genera (Stat et al. 2008) and between closely related congeners (Hoadley et al. 2021; Díaz-Almeyda et al. 2017). For instance, Hoadley et al. uncovered differences in cell density, cell size, chlorophyll concentrations, photosynthetic rates, and photoprotective pathways among *Cladocopium* C15 sub-clades in *P. cylindrica* (Hoadley et al. 2021). Such functional variation suggests that even the minimal symbiont shifting we saw in *P. cylindrica* (Figure 3A) may influence coral performance. However, monitoring results indicate that these shifts are not consistently beneficial (Figure 5).

When examining Symbiodiniaceae shifts in relation to partial mortality 72 weeks after transplantation, colonies with ITS2 profile changes (Figure 4A) experienced slightly worse outcomes (Figure 5E), a pattern driven by *P. lobata*. The increased partial mortality observed with most symbiont shifts (Figure 5E) suggests that retaining the original, C15-dominated assemblage was the most successful strategy. This is further supported by the fact that six out of seven *P. lobata* colonies that maintained this community for at least 18 weeks showed no signs of partial mortality (Figure 5E). Particularly, the predominance of shifts within the *Cladocopium* C15 subtype profiles that led to increased partial mortality raises questions about the ecological role of different C15 sub-clades.

4.3 | Post-Transplantation Appearance of C40, C116, and D1 in *P. lobata*

Although maintenance of C15 dominance seems to be most common in *P. lobata* and the rule for *P. cylindrica*, some of the *P. lobata* colonies sampled harboured novel Symbiodiniaceae taxa, including *Cladocopium* C116 and C40, and *Durusdinium* D1 approximately 18 weeks after transplantation. *Durusdinium* types, known for their stress tolerance (Lesser et al. 2013; Stat and Gates 2011), have been observed dominating the Symbiodiniaceae communities of *Porites* spp. in Kiribati after marine heatwaves (Starko et al. 2023). However, it is somewhat surprising that we see some colonies dominated by *Durusdinium* after transplantation, given the limited sampling timeframe and the fact that these ITS2 types were not detected in any appreciable abundance during initial sampling prior to transplantation. It is possible that these symbionts were present in parts of the tissue that were not sampled for metabarcoding and subsequently spread across tissues of the transplanted fragment (Rouzé et al. 2019; Bollati et al. 2024). Previous studies have described diverse Symbiodiniaceae clades co-occurring in *Porites* colonies (Tan et al. 2020; Terraneo et al. 2019), making this scenario plausible. Alternatively, it is possible that new symbiont types were acquired horizontally from the environment as an acclimatisation response to transplantation. Further, the site which experienced the most significant changes in *P. lobata* Symbiodiniaceae community, West A, is surrounded by large thickets of *Acropora pulchra*, which are known to harbour the newly acquired Symbiodiniaceae clades (e.g., C40) (Anthony, Lock, et al. 2023; Anthony, Lock, Pérez-Rosales, et al. 2024). This hypothesis may be further supported by the observed slight decline in Symbiodiniaceae cell densities following transplantation (Figure 2) and the site-specific shift in West A towards these more phylogenetically distinct clades (Figure 4C).

Cladocopium C40 is dominant in the staghorn coral *Acropora pulchra* in Guam (Anthony, Lock, et al. 2023), whereas *Durusdinium* D1 is dominant in *Pocillopora damicornis* in Guam (Tramonte 2023). Both of these coral species occurred in close proximity to the *Porites* fragments transplanted into the common garden plots, potentially serving as a source for the new Symbiodiniaceae observed in *P. lobata* tissues following transplantation. The *P. lobata* colonies that shifted to *Cladocopium* C40 and *Durusdinium* D1 were found exclusively in a single plot (WA). Considering that clonal fragments were transplanted to all four plots, the observed shifts in Symbiodiniaceae type profiles were likely the result of site-specific acclimatisation. In fact, Anthony et al. transplanted 10 *A. pulchra* colonies (80 fragments) alongside the exact *Porites* corals analysed here (Anthony, Lock, Pérez-Rosales, et al. 2024). These corals were completely dominated by *Cladocopium* C40-C3-C115 type profiles and showed no sign of community shifts following transplantation even 16 months after transplantation. Instead, *A. pulchra* experienced a rapid decline in cell density following transplantation, something we did not see here in *Porites* (Figure 2). Perhaps this could have provided a source for the newly acquired C40. Nonetheless, based on this information, *P. cylindrica* and *P. lobata* almost certainly have different acclimatisation strategies from their co-dominant, faster growing counterpart, *A. pulchra*. Perhaps the shifts in Symbiodiniaceae ITS2 profiles prevented the dynamic symbiotic breakdown observed in co-occurring *A. pulchra*. That said, 16 months after the study, *A. pulchra* had the lowest mortality, followed by *P. lobata*, and then *P. cylindrica* (Anthony, Lock, Pérez-Rosales, et al. 2024).

To better understand the trade-offs of these symbiont community shifts, it will be essential to examine whether such changes in Symbiodiniaceae communities are common on larger scales and directly assess their impact on coral holobiont physiology. Generally, coral restoration focuses on propagating populations of corals that survived prior stress events, such as coral bleaching, with the expectation that these survivor corals possess resilient traits, such as stress-tolerant Symbiodiniaceae communities, that increase their overall resilience (Boström-Einarsson et al. 2020). The shifts in symbiont community observed in the current study suggest that coral-associated Symbiodiniaceae may change dramatically and somewhat stochastically in response to transplantation to different sites, even between congeneric coral species, and minimal changes in abiotic factors (temperature, depth, light availability, nitrogen levels). It is perhaps most interesting that neither host colour morphology nor

host genotype played a considerable role in predicting these endosymbiotic communities nor their response to a new environment (Table 1). Consequently, coral-associated Symbiodiniaceae may change readily and potentially affect the success of coral restoration projects that rely on transplanting corals which possess resilient Symbiodiniaceae clades.

4.4 | Identification of *Parendozoicomonas*-Dominated Bacterial Communities

In addition to Symbiodiniaceae, coral microbiomes are comprised of associations with diverse bacterial communities (Rohwer et al. 2002) that provide a variety of physiological benefits (Voolstra et al. 2024; Raina et al. 2009; Shnit-Orland and Kushmaro 2009; Gilbert et al. 2012) and sometimes detriment (Voolstra et al. 2024; Vega Thurber et al. 2009) to their coral host. Similar to Symbiodiniaceae, certain corals, including *Porites*, are generally known to have high fidelity to particular bacterial associates and exhibit limited flexibility in response to environmental change (Pollock et al. 2018). In this study, we saw nearly all *P. lobata* and *P. cylindrica* fragments dominated by *Endozoicomonadaceae*, a family well known to be the most prevalent bacterial associate in many corals including *Porites* species (Voolstra et al. 2024; Meyer et al. 2014). The precise roles of *Endozoicomonadaceae* taxa in coral holobiont function are still not well understood, but these bacteria are believed to play important roles in coral nutrient cycling (Voolstra et al. 2024; Ding et al. 2016; Pogoreutz et al. 2022; Tandon et al. 2020), harbour high metabolic diversity, and contribute a variety of roles to coral holobiont functioning (Neave et al. 2017). Specifically, Tandon et al. found that coral colonies in close proximity harboured different, but closely related *Endozoicomonas* taxa, which possessed varying levels of reactive oxygen scavenging potential (Tandon et al. 2022).

Given the dominance and the putatively important roles of *Endozoicomonadaceae* in the *Porites* microbiomes surveyed, we used phylogenetic analysis to home in on the identity of ASVs assigned to this family. While ASV data provide advantages over traditional OTU clustering approaches in the analysis of prokaryote diversity and discovery of novel taxa (Fasolo et al. 2024), lower-level taxonomic assignments may be noisy, not least because of potentially missing taxa in reference databases used for assignment of taxonomies (e.g., *Parendozoicomonas* and other recently described *Endozoicomonadaceae* genera are missing from the SILVA database). Based on phylogenetic analysis, over 99.9% of *Endozoicomonas* ASVs were closely related to the genera *Parendozoicomonas* (Figure S4), particularly *Parendozoicomonas haliclonae*, which was the first species described in the genus after its isolation from a marine sponge (Bartz et al. 2018). The diversity and functional roles of the genus *Parendozoicomonas* remain largely undescribed, but given their dominance in this study and the association of their loss with higher partial mortality, *Parendozoicomonas* species may provide their coral host with functional benefits similar to those described for *Endozoicomonas* (Cunning et al. 2015; Epstein et al. 2019) that merit further examination. Similar to *Endozoicomonas*, *Parendozoicomonas* species have been described as dominating *Porites* spp. across large geographic ranges (Hochart et al. 2023). Future research should work to resolve the taxonomy and disentangle the metabolic functions of the widespread *Endozoicomonas* and *Parendozoicomonas* taxa to better understand their relationship to coral holobiont health.

4.5 | Bacterial Community Diversification and Relative *Endozoicomonadaceae* Decline

Studies have reported significant changes in bacterial communities as their coral hosts experience stress events such as eutrophication (Jessen et al. 2013), deoxygenation (Howard et al. 2023) and coral bleaching (Ziegler et al. 2017), but few studies examined the changes associated with transplantation (Ziegler et al. 2017; Strudwick et al. 2022; Haydon et al. 2021). Given the diverse roles that bacterial associates play in coral health, these changes could be major determinants of the fate of the coral holobiont and, ultimately, the success of coral restoration projects. Here, *P. lobata* across all sites showed changes in bacterial communities after transplantation and 18 weeks of acclimatisation (Figure 4D,F). More specifically, we commonly observed a decline in the relative abundance of *Endozoicomonadaceae*. However, the timing of bacterial community shifts varied significantly by individual colony, site, and timepoint (Figures 3B and 4D; Table 1).

The loss of *Endozoicomonadaceae* taxa has been observed in *Porites* corals that displayed disease lesions (Meyer et al. 2014) and experienced declining water quality, whereas both increases and decreases have been observed in response to heat stress (Apprill et al. 2016; McDevitt-Irwin et al. 2019). Studies have observed losses of *Endozoicomonadaceae* (Haydon et al. 2021) in response to coral transplantation, while others have correlated the loss of this bacterial family to declining coral health (Bourne et al. 2008; Ziegler et al. 2016). In this study, we observed reductions in the relative abundance of *Endozoicomonadaceae* (mostly genus *Parendozoicomonas*) in *P. lobata* (Figure 3B), which, interestingly, experienced less than half of the observations of disease over the 18-week experiment compared to *P. cylindrica* (Figure 5B). Associated with this was also the lower long-term survival of *P. lobata* colonies with lower relative abundances of *Endozoicomonadaceae* following transplantation (Figure 5F). Additionally, we found increases in the relative abundance of *Rhodobacteraceae* in both *Porites* spp., but more pronounced in *P. lobata* (Figure 3B). Increases in *Rhodobacteraceae* have been observed as *Endozoicomonas* abundances decline (McDevitt-Irwin et al. 2019; Botté et al. 2022; Deignan and McDougald 2022; Miller and Bentlage 2024) which has been correlated with white syndrome lesions in acroporid corals (Pollock et al. 2017), a disease which we observed increasing in prevalence immediately following transplantation. Despite the lower overall disease prevalence in *P. lobata* (Figure 5B), the reduction of *Endozoicomonadaceae* and increases of *Rhodobacteraceae* relative abundance could represent a stressed and potentially susceptible microbiome (McDevitt-Irwin et al. 2019; Botté et al. 2022; Deignan and McDougald 2022; Miller and Bentlage 2024). Indeed, *P. lobata* samples with higher relative abundance of *Rhodobacteraceae* (and other bacteria) and low relative abundance from *Endozoicomonadaceae* displayed higher susceptibility to transplantation stress, as indicated by higher partial mortality 72 weeks after transplantation (Figure 5F). Further,

purple and brown colour morphs of *P. lobata* harboured significantly different bacterial communities, which have been observed before in *Montipora capitata* (Shore-Maggio et al. 2015). Despite this, we saw no indication that colours were associated with significantly different mortality after being transplanted to new sites (Figure 5A), nor did *P. lobata* colour morphs seem to be more susceptible to disease (Figure 5B). *P. cylindrica* experienced higher disease overall (Figure 5B) despite having a generally less diverse bacterial community than *P. lobata* (Figure 4). *P. cylindrica* mortality was also unrelated to having a diversified bacterial community (Figure 5).

As with changes in Symbiodiniaceae community, it is difficult to untangle whether new bacterial taxa that emerged after transplantation were present in coral tissues during the initial sampling at low abundance or if they represent bacteria from the environment colonising corals after the stress of transplantation. It is also beyond our ability to hypothesise the source of new bacterial taxa, as we do not have data for the bacterial community dynamics of the corals surrounding the transplant sites. It is important to note that variability of relative abundances may not necessarily reflect changes in absolute abundance of bacterial taxa present in coral tissues. Future studies should incorporate approaches to estimate absolute abundances of dominant coral-associated bacteria, for example using qPCR, in addition to DNA metabarcoding, to gain additional insights into bacterial microbiome community dynamics and turnover in response to transplantation. Additionally, bacterial taxa are often localised to specific anatomical areas of corals (Bollati et al. 2024; Miller and Bentlage 2024; Marchioro et al. 2020). Therefore, it is unclear whether our observed changes in the bacterial community occurred across all anatomical areas or within specific tissues. Further research that characterises bacterial microbiome localisation across coral anatomy, through longer periods of time, or with higher temporal resolution could help understand the modes of acquisition and localisation of bacterial taxa that are associated with microbiome turnover following transplantation. Differences in symbiont density, coral colour intensity, and microbial composition between the *Porites* species may partly reflect differences in coral host genotype diversity considering that *P. lobata* was represented by three genotypes in this study whereas *P. cylindrica* was represented by a single genotype. Although this study attempted to capture genotypic variation by sampling distinct colour morphotypes for each species, broader sampling of genotypic diversity in future studies will be essential to further evaluate the influence of host genetics on microbial communities and restoration outcomes.

5 | Conclusions

In this study, we report the transplantation dynamics of the Symbiodiniaceae and bacterial microbiome communities of two dominant reef-building coral species, *P. lobata* and *P. cylindrica*, and their colour morphs. Although closely related coral species, we observed significant differences in their responses to transplantation, in particular pronounced differences in Symbiodiniaceae and bacterial microbiome community dynamics. Both species were dominated by *Cladocopium* C15, but substantial shifts to other *Cladocopium* and *Durusdinium* type profiles were observed in some *P. lobata* colonies. Shifts in Symbiodiniaceae and bacterial communities following transplantation were correlated with higher partial mortality 72 weeks after the initial transplantation of *P. lobata*, but not for *P. cylindrica*. *Parendozoicomonas* dominated the bacterial microbiomes of both species initially, but several colonies of both species saw reductions in relative abundance in *Parendozoicomonas* and the emergence of other bacterial taxa associated with sampling site, species, colony, and coral colour that may be reflective of specific acclimatisation responses. Longer-term monitoring of coral holobiont communities undergoing stressful events such as transplantation will help elucidate if these substantial shifts represent a temporary or permanent shift and identify consistent co-occurrence patterns of bacterial and Symbiodiniaceae taxa. Basic biology is inherently tied to effective management. Therefore, further understanding these dynamics may inform the design and implementation of effective reef management, restoration, and rehabilitation programmes.

Author Contributions

C.L., C.J.A., L.R, and B.B. conceptualization. C.L., T.M., G.M., C.J.A., C.T., L.P., L.R., B.B. investigation. C.L., T.M., C.J.A., J.F., H.R., L.P., L.R., and B.B. methodology. C.L., C.J.A., T.M., H.R., B.B., and J.F. formal analysis. C.L., T.M., C.J.A., G.M., C.T., and L.P. data curation. B.B., L.R., and S.W.D. resources. B.B., L.R., H.R., and S.W.D. supervision. B.B. and L.R. funding acquisition. C.L. and C.J.A. visualization. C.L. and C.J.A. writing – original draft preparation.

Acknowledgements

This work was directly supported by Guam NSF EPSCoR through the National Science Foundation (award OIA-1946352). Open access publishing facilitated by University of Technology Sydney, as part of the Wiley - University of Technology Sydney agreement via the Council of Australian University Librarians.

Conflicts of Interest

The authors declare no conflicts of interest.

Data Availability Statement

16S and ITS2 metabarcoding sequences presented in this study can be found in online repositories. Sequence data were deposited in NCBI GenBank's short read archive (16S: SRR33748254—SRR33748361; ITS2: SRR33748254—SRR33748361), accessible through BioProject PRJNA1211696. R scripts for the analysis conducted were deposited on Github (https://github.com/AnthonyCuog/PoritesCommonGarden).

References

Anthony, C. J., C. Lock, and B. Bentlage. 2023. "Rapid, High-Throughput Phenotypic Profiling of Endosymbiotic Dinoflagellates (Symbiodiniaceae) Using Benchtop Flow Cytometry." *PLoS One* 18: e0290649.

Anthony, C. J., C. Lock, R. Crisostomo, and B. Bentlage. 2024. "Three-Dimensional Modeling of Coral Skeletal Fragments for Morphometrics." *protocols.io* 101060.

Anthony, C. J., C. Lock, G. Pérez-Rosales, et al. 2024. "Symbiodiniaceae Phenotypic Traits as Bioindicators of Acclimatization After Coral Transplantation." *Marine Pollution Bulletin* 209: 117250.

Anthony, C. J., C. Lock, B. M. Taylor, and B. Bentlage. 2023. "Cellular Plasticity Facilitates Phenotypic Change in a Dominant Coral's Symbiodiniaceae Assemblage." *Frontiers in Ecology and Evolution* 11.

Anthony, C. J., G. McDermott, C. Lock, T. Miller, B. Bentlage, and L. J. Raymundo. 2023. "Depth-Independent Phenotypic Variation of Massive *Porites* Coral Color Morphs." *Marine Ecology* 45: e12788. https://doi.org/10.1111/maec.12788.

Apprill, A., S. Mcnally, R. Parsons, and L. Weber. 2015. "Minor Revision to V4 Region SSU rRNA 806R Gene Primer Greatly Increases Detection of SAR11 Bacterioplankton." *Aquatic Microbial Ecology* 75: 129–137.

Apprill, A., L. G. Weber, and A. E. Santoro. 2016. "Distinguishing Between Microbial Habitats Unravels Ecological Complexity in Coral Microbiomes." *Msystems* 1: e00143-16.

Aranda, M., Y. Li, Y. J. Liew, et al. 2016. "Genomes of Coral Dinoflagellate Symbionts Highlight Evolutionary Adaptations Conducive to a Symbiotic Lifestyle." *Scientific Reports* 6: 39734.

Barshis, D. J., J. H. Stillman, R. D. Gates, R. J. Toonen, L. W. Smith, and C. Birkeland. 2010. "Protein Expression and Genetic Structure of the Coral *Porites lobata* in an Environmentally Extreme Samoan Back Reef: Does Host Genotype Limit Phenotypic Plasticity?" *Molecular Ecology* 19: 1705–1720.

Bartz, J. O., J. Blom, H. J. Busse, et al. 2018. "Parendozoicomonas Haliclonae Gen. Nov. sp. Nov. Isolated From a Marine Sponge of the Genus Haliclona and Description of the Family Endozoicomonadaceae Fam. Nov. Comprising the Genera Endozoicomonas, Parendozoicomonas, and Kistimonas." *Systematic and Applied Microbiology* 41: 73–84.

Bates, D., M. Mächler, B. Bolker, and S. Walker. 2015. "Fitting Linear Mixed-Effects Models Using lme4." *Journal of Statistical Software* 67: 1–48.

Berkelmans, R., and M. J. H. Van Oppen. 2006. "The Role of Zooxanthellae in the Thermal Tolerance of Corals: A "Nugget of Hope" for Coral Reefs in an Era of Climate Change." *Proceedings of the Royal Society B: Biological Sciences* 273: 2305–2312.

Bollati, E., D. J. Hughes, D. J. Suggett, J.-B. Raina, and M. Kühl. 2024. "Microscale Sampling of the Coral Gastrovascular Cavity Reveals a Gut-Like Microbial Community." *Animal Microbiome* 6: 55.

Boström-Einarsson, L., R. C. Babcock, E. Bayraktarov, et al. 2020. "Coral Restoration – A Systematic Review of Current Methods, Successes, Failures and Future Directions." *PLoS One* 15: e0226631.

Botté, E. S., N. E. Cantin, V. J. L. Mocellin, et al. 2022. "Reef Location Has a Greater Impact Than Coral Bleaching Severity on the Microbiome of Pocillopora Acuta." *Coral Reefs* 41: 63–79.

Bourne, D., Y. Iida, S. Uthicke, and C. Smith-Keune. 2008. "Changes in Coral-Associated Microbial Communities During a Bleaching Event." *ISME Journal* 2: 350–363.

Burdick, D., L. Raymundo, D. Drake, and A. Hershberger. 2023. "A Decade of Change on Guam's Coral Reefs A Report of Guam Long-Term Coral Reef Monitoring Program Activities Between 2010 and 2021 August 2023."

Cabaitan, P. C., H. T. Yap, and E. D. Gomez. 2015. "Performance of Single Versus Mixed Coral Species for Transplantation to Restore Degraded Reefs." *Restoration Ecology* 23: 349–356.

Callahan, B. J., P. J. McMurdie, M. J. Rosen, A. W. Han, A. J. A. Johnson, and S. P. Holmes. 2016. "DADA2: High-Resolution Sample Inference From Illumina Amplicon Data." *Nature Methods* 13: 581–583.

Casey, J. M., S. R. Connolly, and T. D. Ainsworth. 2015. "Coral Transplantation Triggers Shift in Microbiome and Promotion of Coral Disease Associated Potential Pathogens." *Scientific Reports* 5: 1–11.

Castresana, J. 2000. "Selection of Conserved Blocks From Multiple Alignments for Their Use in Phylogenetic Analysis." *Molecular Biology and Evolution* 17: 540–552.

Ceh, J., M. R. Kilburn, J. B. Cliff, J. B. Raina, M. Van Keulen, and D. G. Bourne. 2013. "Nutrient Cycling in Early Coral Life Stages: *Pocillopora damicornis* Larvae Provide Their Algal Symbiont (Symbiodinium) With Nitrogen Acquired From Bacterial Associates." *Ecology and Evolution* 3: 2393–2400.

Christensen, R. H. B., and M. R. H. B. Christensen. 2015. "Package Ordinal." Stand 19.

Cinner, J. 2014. "Coral Reef Livelihoods." *Current Opinion in Environment Sustainability* 7: 65–71. https://doi.org/10.1016/j.cosust.2013.11.025.

Claar, D. C., K. L. Tietjen, K. D. Cox, R. D. Gates, and J. K. Baum. 2020. "Chronic Disturbance Modulates Symbiont (Symbiodiniaceae) Beta Diversity on a Coral Reef." *Scientific Reports* 10: 4492.

Cunning, R., R. D. Gates, and P. J. Edmunds. 2017. "Using High-Throughput Sequencing of ITS2 to Describe Symbiodinium Metacommunities in St. John, US Virgin Islands." *PeerJ* 5: e3472.

Cunning, R., R. N. Silverstein, and A. C. Baker. 2015. "Investigating the Causes and Consequences of Symbiont Shuffling in a Multi-Partner Reef Coral Symbiosis Under Environmental Change." *Proceedings of the Royal Society B: Biological Sciences* 282: 20141725.

Darriba, D., G. L. Taboada, R. Doallo, and D. Posada. 2012. "jModelTest 2: More Models, New Heuristics and Parallel Computing." *Nature Methods* 9: 772 Go to original source.

de la Vega, P., G. G. Shimpi, and B. Bentlage. 2023. "Genome Sequence of the Endosymbiont Endozoicomonas sp. Strain GU-1 (Gammaproteobacteria), isolated From the Staghorn Coral *Acropora pulchra* (Cnidaria: Scleractinia)." *Microbiology Resource Announcements* 12: e01355-22.

Deignan, L. K., and D. McDougald. 2022. "Differential Response of the Microbiome of Pocillopora Acuta to Reciprocal Transplantation Within Singapore." *Microbial Ecology* 83: 608–618.

Díaz-Almeyda, E. M., C. Prada, A. H. Ohdera, et al. 2017. "Intraspecific and Interspecific Variation in Thermotolerance and Photoacclimation in Symbiodinium Dinoflagellates." *Proceedings of the Royal Society B: Biological Sciences* 284: 20171767.

Ding, J. Y., J. H. Shiu, W. M. Chen, Y. R. Chiang, and S. L. Tang. 2016. "Genomic Insight Into the Host-Endosymbiont Relationship of *Endozoicomonas montiporae* CL-33T With Its Coral Host." *Frontiers in Microbiology* 7: 251.

Dixon, P. 2003. "VEGAN, a Package of R Functions for Community Ecology." *Journal of Vegetation Science* 14: 927–930.

Dougan, K. E., A. J. Bellantuono, T. Kahlke, et al. 2022. "Whole-Genome Duplication in an Algal Symbiont Serendipitously Confers 1 Thermal Tolerance to Corals."

Edgar, R. C. 2004. "MUSCLE: Multiple Sequence Alignment With High Accuracy and High Throughput." *Nucleic Acids Research* 32: 1792–1797.

Epstein, H. E., G. Torda, and M. J. H. van Oppen. 2019. "Relative Stability of the Pocillopora Acuta Microbiome Throughout a Thermal Stress Event." *Coral Reefs* 38: 373–386.

Epstein, N., R. P. M. Bak, and B. Rinkevich. 2001. "Strategies for Gardening Denuded Coral Reef Areas: The Applicability of Using Different Types of Coral Material for Reef Restoration." *Restoration Ecology* 9: 432–442.

Fasolo, A., S. Deb, P. Stevanato, G. Concheri, and A. Squartini. 2024. "ASV vs OTUs Clustering: Effects on Alpha, Beta, and Gamma Diversities in Microbiome Metabarcoding Studies." *PLoS One* 19: e0309065.

Fifer, J. E., V. Bui, J. T. Berg, et al. 2022. "Microbiome Structuring Within a Coral Colony and Along a Sedimentation Gradient." *Frontiers in Marine Science* 8.

Forsman, Z. H., B. Rinkevich, and C. L. Hunter. 2006. "Investigating Fragment Size for Culturing Reef-Building Corals (Porites Lobata and *P. compressa*) in ex situ nurseries." *Aquaculture* 261: 89–97. https://doi.org/10.1016/j.aquaculture.2006.06.040.

Gilbert, J. A., R. Hill, M. A. Doblin, and P. J. Ralph. 2012. "Microbial Consortia Increase Thermal Tolerance of Corals." *Marine Biology* 159: 1763–1771.

Gleason, D. F. 1993. "Differential Effects of Ultraviolet Radiation on Green and Brown Morphs of the Caribbean Coral *Porites astreoides*." *Limnology and Oceanography* 38: 1452–1463.

Gleason, D. F. 1998. "Sedimentation and Distributions of Green and Brown Morphs of the Caribbean Coral *Porites astreoides* Lamarck." *Journal of Experimental Marine Biology and Ecology* 230: 73–89.

Golbuu, Y., R. van Woesik, R. H. Richmond, P. Harrison, and K. E. Fabricius. 2011. "River Discharge Reduces Reef Coral Diversity in Palau." *Marine Pollution Bulletin* 62: 824–831.

Gouy, M., S. Guindon, and O. Gascuel. 2010. "SeaView Version 4: A Multiplatform Graphical User Interface for Sequence Alignment and Phylogenetic Tree Building." *Molecular Biology and Evolution* 27: 221–224.

Grottoli, A. G., P. D. Martins, M. J. Wilkins, et al. 2018. "Coral Physiology and Microbiome Dynamics Under Combined Warming and Ocean Acidification." *PLoS One* 13: e0191156.

Guindon, S., and O. Gascuel. 2003. "A Simple, Fast, and Accurate Algorithm to Estimate Large Phylogenies by Maximum Likelihood." *Systematic Biology* 52: 696–704.

Hauff, B., J. A. Haslun, K. B. Strychar, P. H. Ostrom, and J. M. Cervino. 2016. "Symbiont Diversity of Zooxanthellae (Symbiodinium spp.) in Porites Astreoides and *Montastraea cavernosa* From a Reciprocal Transplant in the Lower Florida Keys." *International Journal of Biology* 8: 9.

Haydon, T. D., J. R. Seymour, J. B. Raina, et al. 2021. "Rapid Shifts in Bacterial Communities and Homogeneity of Symbiodiniaceae in Colonies of Pocillopora Acuta Transplanted Between Reef and Mangrove Environments." *Frontiers in Microbiology* 12: 756091.

Hoadley, K. D., D. T. Pettay, A. Lewis, et al. 2021. "Different Functional Traits Among Closely Related Algal Symbionts Dictate Stress Endurance for Vital Indo-Pacific Reef-Building Corals." *Global Change Biology* 27: 5295–5309.

Hochart, C., L. Paoli, H.-J. Ruscheweyh, et al. 2023. "Ecology of Endozoicomonadaceae in Three Coral Genera Across the Pacific Ocean." *Nature Communications* 14: 3037.

Hothorn, T., K. Hornik, M. A. Van De Wiel, and A. Zeileis. 2008. "Implementing a Class of Permutation Tests: The Coin PackageJournal of Statistical Software."

Howard, R. D., M. D. Schul, L. M. Rodriguez Bravo, A. H. Altieri, and J. L. Meyer. 2023. "Shifts in the Coral Microbiome in Response to in Situ Experimental Deoxygenation." *Applied and Environmental Microbiology* 89: e0057723.

Hughes, T. P., M. L. Barnes, D. R. Bellwood, et al. 2017. "Coral Reefs in the Anthropocene." *Nature* 546: 82–90.

Hume, B. C. C., A. Mejia-Restrepo, C. R. Voolstra, and M. L. Berumen. 2020. "Fine-Scale Delineation of Symbiodiniaceae Genotypes on a Previously Bleached Central Red Sea Reef System Demonstrates a Prevalence of Coral Host-Specific Associations." *Coral Reefs* 39: 583–601.

Hume, B. C. C., E. G. Smith, M. Ziegler, et al. 2019. "SymPortal: A Novel Analytical Framework and Platform for Coral Algal Symbiont Next-Generation Sequencing ITS2 Profiling." *Molecular Ecology Resources* 19: 1063–1080.

Hume, B. C. C., M. Ziegler, J. Poulain, et al. 2018. "An Improved Primer Set and Amplification Protocol With Increased Specificity and Sensitivity Targeting the Symbiodinium ITS2 Region." *PeerJ* 2018: 1–22.

Jessen, C., J. F. Villa Lizcano, T. Bayer, et al. 2013. "In-Situ Effects of Eutrophication and Overfishing on Physiology and Bacterial Diversity of the Red Sea Coral *Acropora hemprichii*." *PLoS One* 8: e62091.

Kenkel, C. D., G. Goodbody-Gringley, D. Caillaud, S. W. Davies, E. Bartels, and M. V. Matz. 2013. "Evidence for a Host Role in Thermotolerance Divergence Between Populations of the Mustard Hill Coral (*Porites astreoides*) From Different Reef Environments." *Molecular Ecology* 22: 4335–4348.

Knowlton, N., R. E. Brainard, R. Fisher, M. Moews, L. Plaisance, and M. J. Caley. 2010. "Coral Reef Biodiversity." In *Life in the World's Oceans*, edited by A.D. McIntyre. https://doi.org/10.1002/9781444325508.ch4.

Korneliussen, T. S., A. Albrechtsen, and R. Nielsen. 2014. "ANGSD: Analysis of Next Generation Sequencing Data." *BMC Bioinformatics* 15: 356.

LaJeunesse, T. C., D. J. Thornhill, E. F. Cox, F. G. Stanton, W. K. Fitt, and G. W. Schmidt. 2004. "High Diversity and Host Specificity Observed Among Symbiotic Dinoflagellates in Reef Coral Communities From Hawaii." *Coral Reefs* 23: 596–603.

Langmead, B., and S. L. Salzberg. 2012. "Fast Gapped-Read Alignment With Bowtie 2." *Nature Methods* 9: 357–359.

Lesser, M. P., K. M. Morrow, and M. S. Pankey. 2019. "N2 Fixation, and the Relative Contribution of Fixed N, in Corals From Curaçao and Hawaii." *Coral Reefs* 38: 1145–1158.

Lesser, M. P., M. Stat, and R. D. Gates. 2013. "The Endosymbiotic Dinoflagellates (Symbiodinium sp.) of Corals Are Parasites and Mutualists." *Coral Reefs* 32: 603–611.

Li, J., Q. Yang, J. Dong, et al. 2022. "Microbiome Engineering: A Promising Approach to Improve Coral Health." *Engineering* 28: 105–116. https://doi.org/10.1016/j.eng.2022.07.010.

Liu, H., T. G. Stephens, R. A. González-Pech, et al. 2018. "Symbiodinium Genomes Reveal Adaptive Evolution of Functions Related to Coral-Dinoflagellate Symbiosis." *Communications Biology* 1: 95.

Lock, C., B. Bentlage, and L. J. Raymundo. 2022. "Calcium Homeostasis Disruption Initiates Rapid Growth After Micro-Fragmentation in the Scleractinian Coral *Porites lobata*." *Ecology and Evolution* 12: e9345.

Lock, C., M. M. Gabriel, and B. Bentlage. 2024. "Transcriptomic Signatures Across a Critical Sedimentation Threshold in a Major Reef-Building Coral." *Frontiers in Physiology* 15: 1303681.

Maor-Landaw, K., and O. Levy. 2016. "Survey of Cnidarian Gene Expression Profiles in Response to Environmental Stressors: Summarizing 20 Years of Research, What Are we Heading for?" In *The Cnidaria, Past, Present and Future*, 523–543. Springer.

Marchioro, G. M., B. Glasl, A. H. Engelen, et al. 2020. "Microbiome Dynamics in the Tissue and Mucus of Acroporid Corals Differ in Relation to Host and Environmental Parameters." *PeerJ* 8: e9644.

Martin, M. 2011. "Cutadapt Removes Adapter Sequences From High-Throughput Sequencing Reads." *EMBnet Journal Technical Notes* 17: 2803–2809.

McDevitt-Irwin, J. M., M. Garren, R. McMinds, R. Vega Thurber, and J. K. Baum. 2019. "Variable Interaction Outcomes of Local Disturbance and El Niño-Induced Heat Stress on Coral Microbiome Alpha and Beta Diversity." *Coral Reefs* 38: 331–345.

McMurdie, P. J., and S. Holmes. 2013. "Phyloseq: An R Package for Reproducible Interactive Analysis and Graphics of Microbiome Census Data." *PLoS One* 8: e61217.

Meyer, J. L., V. J. Paul, and M. Teplitski. 2014. "Community Shifts in the Surface Microbiomes of the Coral *Porites astreoides* With Unusual Lesions." *PLoS One* 9: e100316.

Miller, T. C., and B. Bentlage. 2024. "Seasonal Dynamics and Environmental Drivers of Tissue and Mucus Microbiomes in the Staghorn Coral *Acropora pulchra*." *PeerJ* 12: e17421.

Moriarty, T., W. Leggat, M. J. Huggett, and T. D. Ainsworth. 2020. "Coral Disease Causes, Consequences, and Risk Within Coral Restoration."

Trends in Microbiology 28: 793–807. https://doi.org/10.1016/j.tim.2020.06.002.

Neave, M. J., C. T. Michell, A. Apprill, and C. R. Voolstra. 2017. "Endozoicomonas Genomes Reveal Functional Adaptation and Plasticity in Bacterial Strains Symbiotically Associated With Diverse Marine Hosts." *Scientific Reports* 7: 40579.

Nitschke, M. R., D. Abrego, C. E. Allen, et al. 2024. "The Use of Experimentally Evolved Coral Photosymbionts for Reef Restoration." *Trends in Microbiology* 32, no. 12: 1241–1252. https://doi.org/10.1016/j.tim.2024.05.008.

Page, C. A., E. M. Muller, and D. E. Vaughan. 2018. "Microfragmenting for the Successful Restoration of Slow Growing Massive Corals." *Ecological Engineering* 123: 86–94.

Paulino, L., Jr., C. Anthony, C. Lock, J. Berg, E. K. Duenas, and B. Bentlage. 2023. "Quantify Coral Paling With Grayscale-Normalized Color Intensity Values V1." *protocols.io* 75382.

Pinzón, J. H., B. Kamel, C. A. Burge, et al. 2015. "Whole Transcriptome Analysis Reveals Changes in Expression of Immune-Related Genes During and After Bleaching in a Reef-Building Coral." *Royal Society Open Science* 2: 140214.

Pogoreutz, C., C. A. Oakley, N. Rädecker, et al. 2022. "Coral Holobiont Cues Prime Endozoicomonas for a Symbiotic Lifestyle." *ISME Journal* 16: 1883–1895.

Pollock, F. J., R. McMinds, S. Smith, et al. 2018. "Coral-Associated Bacteria Demonstrate Phylosymbiosis and Cophylogeny." *Nature Communications* 9: 4921.

Pollock, F. J., N. Wada, G. Torda, B. L. Willis, and D. G. Bourne. 2017. "White Syndrome-Affected Corals Have a Distinct Microbiome at Disease Lesion Fronts." *Applied and Environmental Microbiology* 83: e02799-16.

Putnam, H. M., M. Stat, X. Pochon, and R. D. Gates. 2012. "Endosymbiotic Flexibility Associates With Environmental Sensitivity in Scleractinian Corals." *Proceedings of the Royal Society B: Biological Sciences* 279: 4352–4361.

Quast, C., E. Pruesse, P. Yilmaz, et al. 2012. "The SILVA Ribosomal RNA Gene Database Project: Improved Data Processing and Web-Based Tools." *Nucleic Acids Research* 41: D590–D596.

Raina, J. B., D. Tapiolas, B. L. Willis, and D. G. Bourne. 2009. "Coral-Associated Bacteria and Their Role in the Biogeochemical Cycling of Sulfur." *Applied and Environmental Microbiology* 75: 3492–3501.

Raymundo, L. J., D. Burdick, W. C. Hoot, et al. 2019. "Successive Bleaching Events Cause Mass Coral Mortality in Guam, Micronesia." *Coral Reefs* 38: 677–700. https://doi.org/10.1007/s00338-019-01836-2.

Rohwer, F., V. Seguritan, F. Azam, and N. Knowlton. 2002. "Diversity and Distribution of Coral-Associated Bacteria." *Marine Ecology Progress Series* 243: 1–10.

Rouzé, H., G. Lecellier, X. Pochon, G. Torda, and V. Berteaux-Lecellier. 2019. "Unique Quantitative Symbiodiniaceae Signature of Coral Colonies Revealed Through Spatio-Temporal Survey in Moorea." *Scientific Reports* 9: 7921.

Satoh, N., K. Kinjo, K. Shintaku, et al. 2021. "Color Morphs of the Coral, *Acropora tenuis*, Show Different Responses to Environmental Stress and Different Expression Profiles of Fluorescent-Protein Genes." *G3: Genes, Genomes, Genetics* 11: jkab018.

Shnit-Orland, M., and A. Kushmaro. 2009. "Coral Mucus-Associated Bacteria: A Possible First Line of Defense." *FEMS Microbiology Ecology* 67: 371–380.

Shoguchi, E., C. Shinzato, T. Kawashima, et al. 2013. "Draft Assembly of the Symbiodinium Minutum Nuclear Genome Reveals Dinoflagellate Gene Structure." *Current Biology* 23: 1399–1408.

Shore-Maggio, A., C. M. Runyon, B. Ushijima, G. S. Aeby, and S. M. Callahan. 2015. "Differences in Bacterial Community Structure in Two Color Morphs of the Hawaiian Reef Coral *Montipora capitata*." *Applied and Environmental Microbiology* 81: 7312–7318.

Stamatakis, A. 2014. "RAxML Version 8: A Tool for Phylogenetic Analysis and Post-Analysis of Large Phylogenies." *Bioinformatics* 30: 1312–1313.

Starko, S., J. E. Fifer, D. C. Claar, et al. 2023. "Marine Heatwaves Threaten Cryptic Coral Diversity and Erode Associations Among Coevolving Partners." *Science Advances* 9: eadf0954.

Stat, M., and R. D. Gates. 2011. "Clade D Symbiodinium in Scleractinian Corals: A "Nugget" of Hope, a Selfish Opportunist, an Ominous Sign, or all of the Above?" *Journal of Marine Biology* 2011: 1–9.

Stat, M., W. K. W. Loh, T. C. LaJeunesse, O. Hoegh-Guldberg, and D. A. Carter. 2009. "Stability of Coral-Endosymbiont Associations During and After a Thermal Stress Event in the Southern Great Barrier Reef." *Coral Reefs* 28: 709–713. https://doi.org/10.1007/s00338-009-0509-5.

Stat, M., E. Morris, and R. D. Gates. 2008. "Functional Diversity in Coral-Dinoflagellate Symbiosis." *Proceedings of the National Academy of Sciences of the United States of America* 105: 9256–9261.

Strudwick, P., J. Seymour, E. F. Camp, et al. 2022. "Impacts of Nursery-Based Propagation and Out-Planting on Coral-Associated Bacterial Communities." *Coral Reefs* 41: 95–112.

Sussman, M., B. L. Willis, S. Victor, and D. G. Bourne. 2008. "Coral Pathogens Identified for White Syndrome (WS) Epizootics in the Indo-Pacific." *PLoS One* 3: e2393.

Tan, Y. T. R., B. J. Wainwright, L. Afiq-Rosli, et al. 2020. "Endosymbiont Diversity and Community Structure in *Porites lutea* From Southeast Asia Are Driven by a Suite of Environmental Variables." *Symbiosis* 80: 269–277.

Tandon, K., Y.-J. Chiou, S.-P. Yu, et al. 2022. "Microbiome Restructuring: Dominant Coral Bacterium Endozoicomonas Species Respond Differentially to Environmental Changes." *MSystems* 7: e0035922.

Tandon, K., C. Y. Lu, P. W. Chiang, et al. 2020. "Comparative Genomics: Dominant Coral-Bacterium Endozoicomonas Acroporae Metabolizes Dimethylsulfoniopropionate (DMSP)." *ISME Journal* 14: 1290–1303.

Team RC. 2013. *R: A Language and Environment for Statistical Computing*. Foundation for Statistical Computing.

Terraneo, T. I., M. Fusi, B. C. C. Hume, et al. 2019. "Environmental Latitudinal Gradients and Host-Specificity Shape Symbiodiniaceae Distribution in Red Sea Porites Corals." *Journal of Biogeography* 46: 2323–2335.

Tisthammer, K. H., E. Timmins-Schiffman, F. O. Seneca, B. L. Nunn, and R. H. Richmond. 2021. "Physiological and Molecular Responses of Lobe Coral Indicate Nearshore Adaptations to Anthropogenic Stressors." *Scientific Reports* 11: 1–11.

Tramonte, C. A. 2023. Coral Species Replacements on Guam's Reef Flats: Investigating the Role of Symbiodiniaceae Dynamics and Environmental Stressors.

van Oppen, M. J. H., and L. L. Blackall. 2019. "Coral Microbiome Dynamics, Functions and Design in a Changing World." *Nature Reviews Microbiology* 17: 557–567. https://doi.org/10.1038/s41579-019-0223-4.

Vega Thurber, R., D. Willner-Hall, B. Rodriguez-Mueller, et al. 2009. "Metagenomic Analysis of Stressed Coral Holobionts." *Environmental Microbiology* 11: 2148–2163.

Venables, W. N., and B. D. Ripley. 2013. *Modern Applied Statistics With S-PLUS*. Springer Science & Business Media.

Voolstra, C. R., J. B. Raina, M. Dörr, et al. 2024. "The Coral Microbiome in Sickness, in Health and in a Changing World." *Nature Reviews Microbiology* 22: 460–475. https://doi.org/10.1038/s41579-024-01015-3.

Walters, W., E. R. Hyde, D. Berg-Lyons, et al. 2016. "Improved Bacterial 16S rRNA Gene (V4 and V4-5) and Fungal Internal Transcribed Spacer

Marker Gene Primers for Microbial Community Surveys." *MSystems* 1: e00009-15.

Wang, S., E. Meyer, J. K. Mckay, and M. V. Matz. 2012. "2b-RAD: A Simple and Flexible Method for Genome-Wide Genotyping." *Nature Methods* 9: 808–810.

Willis, B. L., C. A. Page, and E. A. Dinsdale. 2004. "Coral Disease on the Great Barrier Reef." In *Coral Health and Disease*, 69–104. Springer.

Xiao, L., S. Johansson, S. Rughöft, et al. 2022. "Photophysiological Response of Symbiodiniaceae Single Cells to Temperature Stress." *ISME Journal* 16: 2060–2064.

Zhenyu, X., K. Shaowen, H. Chaoqun, Z. Zhixiong, W. Shifeng, and Z. Yongcan. 2013. "First Characterization of Bacterial Pathogen, *Vibrio alginolyticus*, for *Porites andrewsi* White Syndrome in the South China Sea." *PLoS One* 8: e75425.

Ziegler, M., C. G. B. Grupstra, M. M. Barreto, et al. 2019. "Coral Bacterial Community Structure Responds to Environmental Change in a Host-Specific Manner." *Nature Communications* 10: 3092.

Ziegler, M., A. Roik, A. Porter, et al. 2016. "Coral Microbial Community Dynamics in Response to Anthropogenic Impacts Near a Major City in the Central Red Sea." *Marine Pollution Bulletin* 105: 629–640.

Ziegler, M., F. O. Seneca, L. K. Yum, S. R. Palumbi, and C. R. Voolstra. 2017. "Bacterial Community Dynamics Are Linked to Patterns of Coral Heat Tolerance." *Nature Communications* 8: 14213.

Supporting Information

Additional supporting information can be found online in the Supporting Information section. **Data S1:** Supporting Information. **Figure S1:** (A) An example map of the randomised layout of one of the four common garden plots. AP = *Acropora pulchra*, PL = *Porites lobata*, PC = *Porites cylindrica*. (B) Replicate fragments were carefully placed next to one another with approximately 10 cm between each coral colony. **Figure S2:** (A) Hourly temperature averages for east and west plots over the sampling period. (B) Daily light (lux) for east and west plots over the sampling period. (C) Water depth (m) for east and west plots over the sampling period. **Figure S3:** Clone dendrograms from the 2b-rad sequencing data from all colonies of *Porites lobata* (PL; B & P for Brown and Purple) and *Porites cylindrica* (PC; B & Y for brown and yellow). Technical replicates of PLP4 delineate the clonal threshold; pairs that fall below this (highlighted in yellow) are suspected clones and not used for microbiological sampling. **Figure S4:** Maximum likelihood (ML) phylogeny of mitochondrial 16S ASVs (bold) assigned to *Endozoicomonadaceae* and publicly available sequence data spanning the described diversity of *Endozoicomonadaceae* (GenBank accession numbers provided in the figure). The ML phylogeny was inferred under a GTR + I + G model; scale bar indicates substitutions per site. Bootstrap values less than 50 are indicated by <. **Figure S5:** General partial mortality trends of *P. cylindrica* (PC) and *P. lobata* (PL) colour morphologies throughout the experiment across all plots: East A, East B, West A, West B.